**Pacific Northwest
National Laboratory**
Operated by Battelle for the
U.S. Department of Energy

Drying Results of K-Basin Fuel Element 6513U (Run 8)

B. M. Oliver   S. C. Marschman
G. S. Klinger   P. J. MacFarlan
J. Abrefah   G. A. Ritter

July 1999

Drying Results of K-Basin Fuel Element 6513U (Run 8)

B. M. Oliver   S. C. Marschman
G. S. Klinger   P. J. MacFarlan
J. Abrefah   G. A. Ritter

July 1999

Pacific Northwest National Laboratory
Richland, Washington 99352

DISCLAIMER

Portions of this document may be illegible in electronic image products. Images are produced from the best available original document.

Summary

An N-Reactor outer fuel element that had been stored underwater in the Hanford 100 Area K-West Basin has been subjected to a combination of low- and high-temperature vacuum drying treatments. These studies are part of a series of tests being conducted by Pacific Northwest National Laboratory on the drying behavior of spent nuclear fuel elements removed from both the K-West and K-East Basins.

The drying test series was designed to test fuel elements that ranged from intact to severely damaged. The fuel element discussed in this report was removed from K-West canister 6513U in 1996 and has remained in wet storage in the Postirradiation Testing Laboratory (PTL, 327 Building) since that time. The fuel element was damaged on both ends. One end was only moderately cracked and damaged, the other severely damaged. K-West canisters can hold up to seven complete fuel assemblies, but, for the purpose of the report, the element is referred to as Element 6513U. Relative to other damaged fuel elements tested, this element had more corrosion at one end, but somewhat less cracking of the outer cladding.

The drying test was conducted in the Whole Element Furnace Testing System located in G-Cell within the PTL. This test system is composed of three basic systems: the in-cell furnace equipment, the system gas loop, and the analytical instrument package. Element 6513U was subjected to drying processes based on those proposed under the Integrated Process Strategy, which included a hot drying step. The test cycles are listed below:

- Cold Vacuum Drying (CVD) at ~50°C under vacuum (~20 hr)

- Pressure Rise Test at ~50°C (~1 hr)

- Hot Vacuum Drying (HVD) for a total of ~75 hr (~19 hr at ~75°C, ~35 hr at ~75°C to ~400°C, and ~21 hr at ~400°C)

- System Cooldown to ~50°C (~64 hr)

- Post-Test Pressure Rise Test at ~50°C (~1 hr).

Prior to CVD, ~10 ml of water were added to the system in addition to the water already on the surface of the fuel element to ensure the element was damp at the start of the test. Approximately 6 ml of water were observed in the condenser during the condenser pumpdown phase of CVD, somewhat higher than a value of 3 g calculated over the same time period from the argon flow and moisture data. Review of previous drying test data suggested that the cause of the incomplete water recovery in the condenser was due to the shorter duration of the condenser pumpdown phase combined with hang-up of water in colder sections of the system. Run 7 (Element 2660M), which had a much longer condenser phase, showed significantly higher fractional water recovery.

Observed pressure rise during the post-CVD Pressure Rise Test was ~0.12 Torr/hr, well below the acceptance criterion of 0.5 Torr/hr. Similar to earlier tests, the total pressure rise observed in the post-CVD test was only partially caused by residual moisture, suggesting that other sources of gas are responsible for some of the total pressure rise observed in that test. Approximately 0.3 mg of water was calculated to have been removed during the Pressure Rise Test. This water can likely be interpreted as coming from free water that was trapped and not completely removed during CVD.

Water removal during the three phases of HVD was ~0.6 g, ~0.3 g, and ~0.014 g, respectively. A main water release peak was observed during HVD-2 at ~134°C. Approximately 4 mg of water were released during post-HVD cooldown, indicating small residual quantities of water remaining even after the drying test was completed. Water released during HVD-1 is attributed largely to the release of water from regions beneath the cladding and from under the corroded regions, with some release possibly from decomposition of metal oxy-hydrates. Water release during HVD-2 is probably from chemisorbed sites (i.e., hydrated species) at higher temperatures. As observed in previous drying tests, a temperature above 400°C may be required for complete drying of the fuel element within a reasonable period of time.

Hydrogen was observed during the test during the condenser pumpdown phase of CVD and during HVD. Hydrogen observed during CVD was ~3 mg, and the data suggest that about 1% or less of the available water released during CVD is oxidizing the fuel. During HVD, hydrogen was first observed at the beginning of HVD-1, reaching a peak at ~0.2 Torr·l/min before slowly decreasing. Approximately ~17 mg of hydrogen were released during HVD-1, attributed largely to oxidation of the fuel by remaining free water. Hydrogen release increased again during HVD-2, with three noticeable peaks at ~148°C (~57 mg), 208°C (~30 mg), and ~257°C (~116 mg). The first two peaks roughly correlate with a similar water release and are likely due to oxidation of fuel by water released through oxy-hydrate decomposition. The third release peak ~ 257°C is likely due to uranium hydride decomposition and represents about 9 g of UH_3. Above ~257°C, the level of hydrogen decreased rapidly, with ~2.7 mg of hydrogen being released during HVD-3. Total hydrogen release during HVD was ~220 mg.

The general drying characteristics for Element 6513U are similar to those observed for Elements 5744U (Run 4) and 1164M (Run 6).

Quality Assurance

This work was conducted under the Quality Assurance Program, Pacific Northwest National Laboratory (PNNL) SNF-70-001, *SNF Quality Assurance Program*, as implemented by the PNNL *SNF Characterization Project Operations Manual*. This QA program has been evaluated and determined to effectively implement the requirements of DOE/RW-0333P, Office of Civilian Radioactive Waste Management *Quality Assurance Requirements and Description (QARD)*. Compliance with the QARD is mandatory for projects that generate data used to support the development of a permanent High-Level Nuclear Waste repository. Further, the U.S. Department of Energy has determined that the testing activities which generated the results documented in this report shall comply with the QARD. Supporting records for the data in this report are located in the permanent PNNL SNF Characterization Project records, *Furnace Testing of SNF Fuel Element 6513U.*

Contents

Figures

Tables

Acronyms

ATS Applied Test Systems

CVD Cold Vacuum Drying

DACS data acquisition and control system

DP dew point

ET elapsed time

GC gas chromatograph

HP Hewlett Packard

HVD Hot Vacuum Drying

ID inside diameter

IPS Integrated Process Strategy

MS mass spectrometer

NIST National Institute of Standards and Technology

OD outside diameter

PNNL Pacific Northwest National Laboratory

PTL Postirradiation Testing Laboratory

QA Quality Assurance

QARD Quality Assurance Requirements and Description

SFEC single fuel element canister

SNF spent nuclear fuel

UHP ultra high purity

VP vapor pressure

1.0 Introduction

The water-filled K-Basins in the Hanford 100 Area have been used to store N-Reactor spent nuclear fuel (SNF) since the 1970s. Because some leaks in the basin have been detected and some of the fuel is breached due to handling damage and corrosion, efforts are underway to remove the fuel elements from wet storage. An Integrated Process Strategy (IPS) has been developed to package, dry, transport, and store these metallic uranium fuel elements in an interim storage facility on the Hanford Site (WHC 1995). Information required to support the development of the drying processes, and the required safety analyses, is being obtained from characterization tests conducted on fuel elements removed from the K-Basins. A series of whole element drying tests (reported in separate documents, see Section 8.0) have been conducted by Pacific Northwest National Laboratory (PNNL)[a] on several intact and damaged fuel elements recovered from both the K-East and K-West Basins.

This report documents the results of the eighth of those tests, which was conducted on an N-Reactor outer fuel element removed from K-West canister 6513U. This element (referred to as Element 6513U) was stored underwater in the K-West Basin from 1983 until 1996. Element 6513U was subjected to a combination of low- and high-temperature vacuum drying treatments that were intended to mimic, wherever possible, the fuel treatment strategies of the IPS. The system used for the drying test was the Whole Element Furnace Testing System, described in Section 2.0, located in the Postirradiation Testing Laboratory (PTL, 327 Building). The test conditions and methodologies are given in Section 3.0. Inspections of the fuel element before and after the test are provided in Section 4.0. The experimental results are provided in Section 5.0 and discussed in Section 6.0.

(a) Operated by Battelle for the U.S. Department of Energy under Contract DE-AC06-76RLO 1830.

2.0 Whole Element Furnace Testing System

A complete description for the Whole Element Furnace Testing System, including detailed equipment specifications, is provided in Ritter et al. (1998).

2.1 Major Systems Overview

An overview of the furnace testing system is presented in this section. The subsystems pertinent to this test report are as follows:

- Vacuum Pumping System – This system consists of a scroll-type vacuum pump, a condenser with chiller, filters, valves, and piping, which provide the vacuum pressures and flows required for the proposed IPS vacuum processes.

- Process Heating System – This system consists of a resistively heated, clam-shell furnace and a sample chamber (retort) to provide heating to the fuel element and to control process temperatures.

- Gas Supply/Distribution System – This system consists of gas bottles; mass flow controllers; piping; and valves for metering argon, air, or oxygen through the system. A bubbler is also available for adding water vapor to the system if desired.

- Gas Analysis Instrumentation – The gas analysis instrumentation includes a 300-amu quadrupole mass spectrometer (MS) and a gas chromatograph (GC) for monitoring selected elements in the process gas stream.

- Process Instrumentation – The system is equipped with several instruments for measuring process temperatures, pressures, and moisture level. An auxiliary turbo vacuum pumping system provides low system pressures for zero adjustment of the high accuracy retort pressure sensor.

- Data Acquisition and Control System (DACS) – The DACS consists of an IBM-compatible computer and data acquisition/control unit to monitor/store key system parameters (temperatures, pressures, flows, moisture level), along with controlling the process heating system and a safety argon system.

Figures 2.1 and 2.2 are photographs of the equipment located inside and outside of G-Cell. The furnace (including retort) and some of the process piping, instrumentation, and valves are located inside the hot cell. The furnace sits on the cell floor, and the process piping is routed to a rack that hangs on the west cell wall. Process piping, electrical power, and instrumentation wires pass through several split plugs on the west side of the cell. The process piping on the outside of the cell is contained within a glove bag, which provides a secondary containment as a precaution in case the process piping lines become contaminated. The vacuum pump, condenser, bubbler, GC, and the remainder of the instrumentation and valves are located inside this glove bag. Instrumentation and electrical power wires are routed through pass-through sleeves on the sides of the glove bag to the instrument rack and computer console.

Figure 2.1. Fuel Element Drying System Components (in-cell)
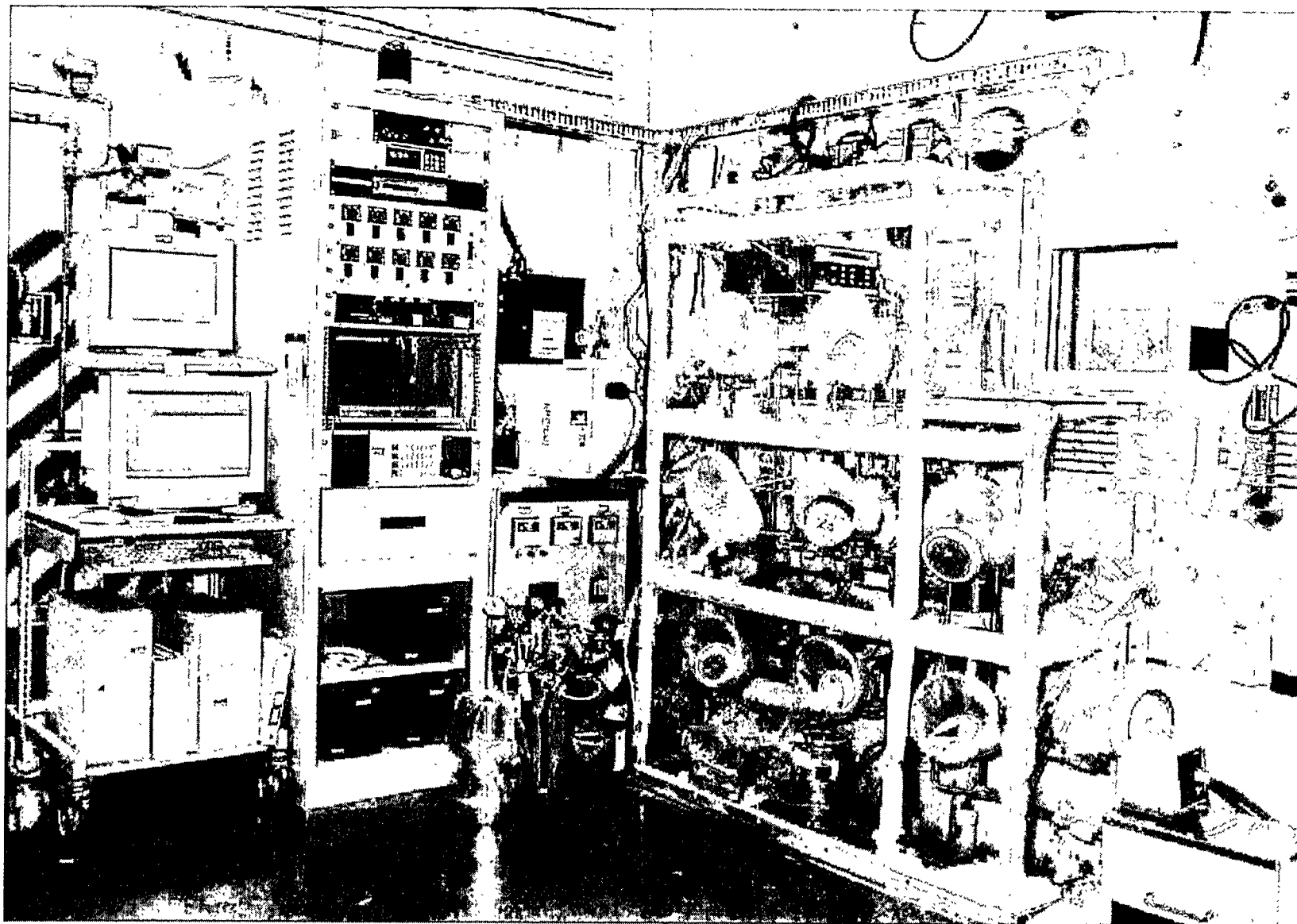
Figure 2.2. Fuel Element Drying System Components (ex-cell)

The instrument rack contains the readout/control units for the pressure sensors, moisture sensor, and flow controllers, along with the heat trace temperature controllers, data acquisition/control unit, turbo pump controller, GC laptop computer, and uninterruptible power supplies. The computers for the DACS and MS are located next to the instrument rack. The following sections provide more detailed descriptions of the components for these subsystems.

2.2   Vacuum Pumping System

The vacuum pumping system provides the pressures and flows required for the proposed IPS processes. This system connects the furnace retort with all the other components of the test system through various valves, fittings, and piping. The vacuum pumping system consists of the following components:

- scroll pump for evacuating the system to pressures below 1 Torr

- water condenser with refrigerated chiller for gross removal of water

- valves and piping for connecting the various components and controlling the flow direction

- particulate filters to prevent the spread of contamination

- heating cords with temperature controllers for preventing condensation in lines.

2.2.1   Varian Scroll Pump

The system vacuum pump is a Varian model 300DS scroll pump. This pump has an ultimate vacuum pressure less than 10^{-2} Torr and a peak pumping speed of 250 l/min (8.8 cfm). These pressures and flows are more than adequate for simulating the conditions of the proposed IPS vacuum processes. For a single fuel element, this amount of flow may be more than desired. Therefore, a metering valve was installed on the pump inlet to throttle the flow to lower levels as required. The desired system pressure is achieved by either using the metering valve or flowing ultra high purity (UHP) argon into the system through the entire gas loop or via a direct injection of ballast gas at the pump inlet. The use of argon gas helps to prevent the in-leakage of moisture-containing air through small system leaks (which are difficult to eliminate) that would interfere with process monitoring equipment.

2.2.2   Water Condenser

The scroll vacuum pump can be damaged by condensation of liquid water in the scroll mechanism, and, since each element was wet at the start of each test, the possibility of pump damage was considered. A water condenser with corresponding chiller was installed in the system to condense the bulk of the water before it reaches the pump. This condenser can be valved into the system in series with the scroll vacuum pump or can be bypassed if not needed. The condenser cannot trap all the liberated free water, but is efficient at removing the majority of free water in the system. The condenser is only used during

the first phase of a Cold Vacuum Drying (CVD) test for a single fuel element. The condenser was custom fabricated specifically for this system. Detailed sketches and specifications for the condenser are given in Ritter et al. (1998). An MKS Baratron model 626-pressure transducer is incorporated into the system to accurately measure and record the outlet pressure of the condenser. This transducer is coupled to an MKS model PDR-C-2C two-channel power supply/readout unit.

2.2.3 Piping, Valves, and Filters

The vacuum pumping system connects the system components through various valves, fittings, and piping. A simplified piping schematic for the system is shown in Figure 2.3. This schematic shows the basic flow path of gases through the system that was used for this test, along with the relative locations of the major components, valves, and instruments. Detailed system piping diagrams are provided in Ritter et al. (1998), along with approximate lengths for the piping lines. As seen in Figure 2.3, there are numerous valves in the system that are used to direct the flow to and from the various components. Most of the valves in the system are ball valves and range from 1/4 in. to 1/2-in. nominal size. The system piping is constructed of thin wall tubing (1/4 in. to 1/2 in. OD) and is typically connected using simple Swagelok fittings (tees, elbows, unions, etc.). Ports for gas sampling/analysis and monitoring of system pressure, temperature, and humidity are also provided at key locations in the system piping. Special fittings and pipe-threaded fittings are used in some locations for connecting piping to the process instruments.

Particulate filters are installed in the system on both the inlet and outlet to the retort to help prevent the spread of contamination to the system piping on the outside of the hot cell. These filters are constructed of a microporous fiberglass media in a stainless steel housing. They are 99.9% efficient for particulates that are 0.2 microns and larger in size. Two different size filters, manufactured by Matheson, are used in the system.

2.2.4 System Line Heaters

All of the stainless steel tubing that carries gases into the furnace retort and resultant gases from the retort is heated to about 75°C to ensure condensable water vapor remains in the gas phase. Simple heat "cords" capable of being wrapped upon each other (as required at tees, elbows, and other connections) were found to be a good heating method for this system. The heating cords are controlled by simple proportional controllers. Type-K thermocouples are installed on each heated line so the DACS can be used to monitor and record temperature.

2.3 Process Heating System

The whole element furnace is a 4-ft-long, resistively heated, clam-shell furnace. The furnace, a Series 3210 supplied by Applied Test Systems (ATS), has a temperature rating of 900°C and total heating capacity of 13,800 W. The internal dimensions are 5 in. ID by 45 in. long. The furnace has three separate sets of heating elements that allow the heating to be controlled in zones; each zone is 15 in. long and supplies up to 4600 W heating. The zones can be controlled separately to establish a flat temperature profile within the furnace, even though heat is lost preferentially out the end with the retort entry flange.
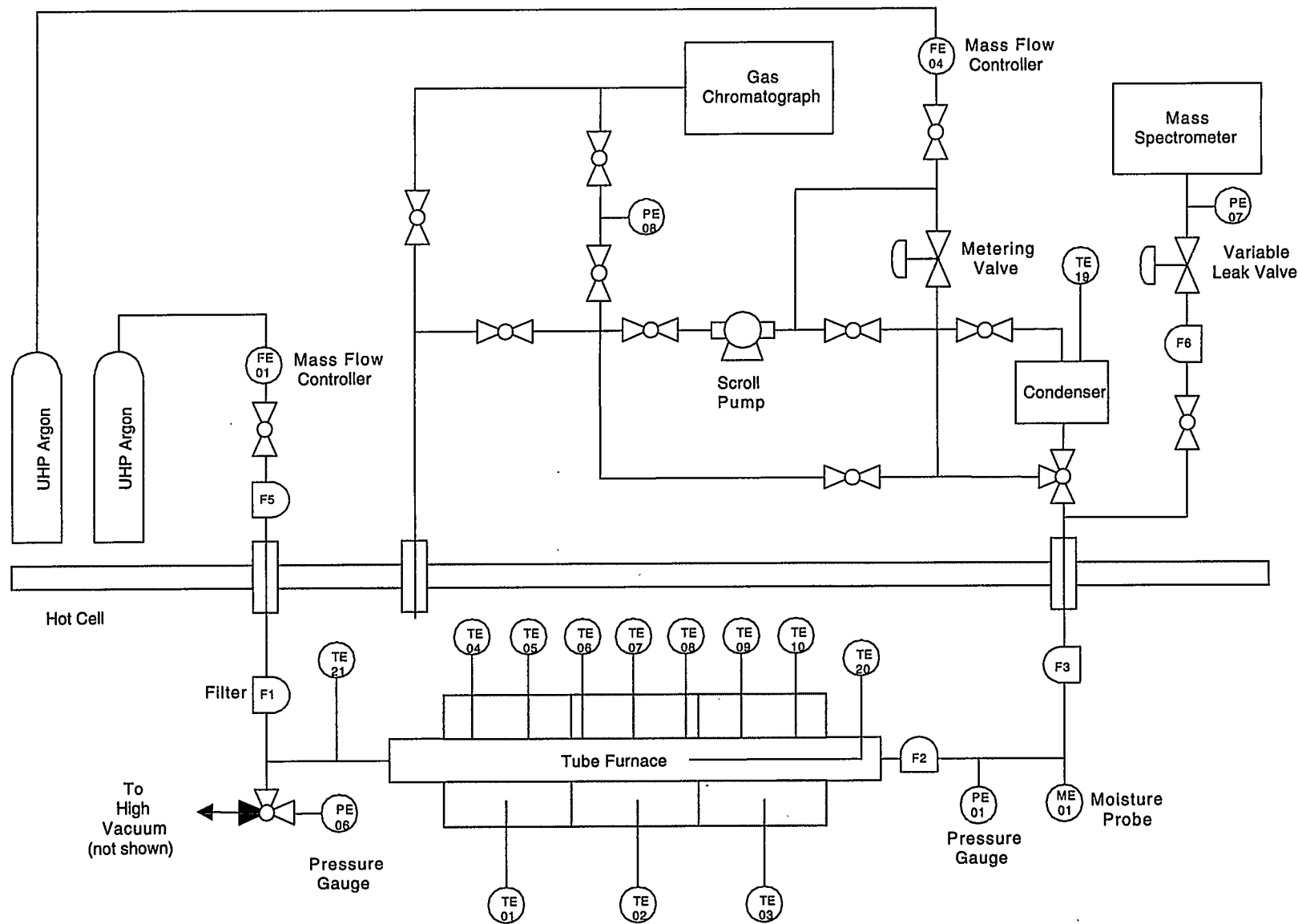
Figure 2.3. Generalized View of Test System

A heat reflector consisting of several thin Inconel plates is used to reduce heat loss from the flange end of the retort. The furnace controller is an ATS Series 3000, which consists of three programmable, self-tuning proportional with integral and derivative controllers. These controllers are also interfaced to the DACS, which is capable of providing limited input to the controllers as required.

The retort, an ATS Series 3910, is an Inconel tube fitted with a gas inlet tube at one end and a gasketed flange at the other. Of all high-temperature materials, Inconel series 600 was selected to reduce the amount of oxidation and water pickup by the retort and associated components. Experience has shown that stainless steel components were easily affected by corrosion, which could then affect test results. The body of the retort is fabricated from schedule 40 Inconel pipe (4.5 in. OD, 4.026 in. ID), and the inside length is about 44.5 in. Seven type-K thermocouples are installed equidistant along one side of the retort and extend into the retort interior approximately 1/8 in. These thermocouples are used to monitor the retort temperature so that if a reaction with the fuel element occurs (which would locally raise the retort temperature), this event can be correlated with the approximate location on the fuel.

An Inconel sample/transfer boat is used to load the fuel element into the furnace. The boat is fabricated from an 11-gauge (0.120-in.-thick) Inconel 601 sheet, which is formed into a flattened u-shape. The boat has a weir and a swivel handle on each end. The weirs are used to keep free water or particulates contained in the boat as required.

2.4 Gas Supply/Distribution System

The gas supply system and vacuum pumping system together are capable of controlling the fuel element environment to vacuum or moderate pressure conditions, and/or exposing the fuel element to a variety of gases or gas mixtures. The gas loop is typically operated as a single-pass system with no capability for recirculation. The gas supply system consists of gas bottles; mass flow controllers; piping; and valves for metering argon, air, or oxygen through the system. A bubbler is also available for adding water vapor to the process gas stream as required, but it was not used in these tests.

The gas supply system contains three Matheson mass flow controllers calibrated for argon, air, and oxygen. All gases are typically specified "ultra high purity" and are additionally filtered for water using molecular sieve columns. Argon is the principal inert gas used, as it is denser than air; provides reasonable thermal conductivity; and requires simpler handling procedures than lighter gases such as helium. The argon purge gas is introduced into the retort through FE-01, which is a Matheson model 8272-0422 oxygen controller, recalibrated for argon gas at 0°C using a NIST-traceable bubble flow meter. The recalibration resulted in a flow rate range of 0 - 304 sccm argon. Air and oxygen are not currently used because any oxidative steps have been deleted from the current IPS for the SNF. The manufacturer's specifications for the air and oxygen controllers' flow rate ranges are 0 - 1000 sccm air and 0 - 10 sccm oxygen. If higher flow rates are desired, a new mass flow controller with a higher range could be procured and installed in the system.

2.5 Gas Analysis Instrumentation

2.5.1 Balzers Omnistar Mass Spectrometer

The Balzers Omnistar MS is a compact, computer-controlled, quadrupole MS capable of scanning to 300 amu. The unit is capable of monitoring up to 64 components within a gas stream with a nominal detection limit of less than 1 ppm for most gases other than hydrogen. The MS was used to monitor hydrogen, nitrogen (for air in-leakage), krypton, xenon, and other elements during the test.

The MS was modified as a result of early system testing and calibration to improve the time response to small changes in hydrogen pressure. Before testing, the MS was calibrated for hydrogen using mixtures of hydrogen and helium, and hydrogen and argon gas. The residence time of each gas could be measured in the quadrupole chamber, and it was observed that the hydrogen decay time was approximately four times as long as helium. This was not unexpected as turbomolecular pumps have a lower pumping efficiency for very light gases. In standard practice this is acceptable, but for these tests, where determining hydrogen could be very important, steps were taken to improve the hydrogen decay time. The MS vacuum system was modified by adding a stainless steel flanged tee, a gate valve, and a room-temperature hydrogen getter downstream from the quadrupole. Under vacuum, the gate valve can be opened, exposing the getter to the system to help scavenge hydrogen from the system following analysis. This modification reduced the residence time of hydrogen in the system substantially and decreased the background level of hydrogen by about a factor of 2. The getter improved the system response to transient events that might result in the release of hydrogen.

A Granville-Phillips variable leak valve, series 203, was added to the gas-sampling inlet of the MS to permit operation over a wide range of system pressures. Without the leak valve, system pressures above about 40 Torr produce too much flow through the MS capillary tube, which overwhelms the turbo pump used to pump down the MS vacuum chamber. Flow through the leak valve can be continuously varied from 0.4 l/s to 10^{-11} l/s, which allows the MS inlet pressure to be controlled to any pressure desired, even if the system pressure varies dramatically. The pressure on the low-pressure side of the leak valve was measured and recorded by the DACS using a second MKS Baratron model 626 transducer (PE-07) combined with the MKS model PDR-C-2C two-channel power supply/readout unit discussed above. The MS was calibrated at ~15 Torr head pressure with four certified gas standards consisting of 10^2, 10^3, 10^4, and 10^5 ppmv hydrogen in argon.

2.5.2 MTI M200 Gas Chromatograph

The MTI M200 Gas Chromatograph is a high-speed GC that is used to monitor the quantities of hydrogen and other light gases in the furnace testing system gas loop. This instrument is interfaced with a laptop computer to record data. The GC is designed to operate at near-atmospheric pressure; thus, it may be configured in two different ways for measurement purposes. At system pressures near atmospheric, the GC is configured to sample directly from the gas loop ahead of the system vacuum pump. When the system is under vacuum, the GC is configured to sample from the exhaust side of the vacuum pump. The

gas output from the pump is sufficiently compressed that the GC can sample and analyze this gas. The GC inlet pressure is measured using a Cole-Parmer pressure sensor (PE-08) and recorded by the DACS. No correction for the difference in the sample pressure and calibration pressure is applied, since both are ~760 Torr (1 atm). The GC was calibrated using the same four gas standards discussed above that were used for the MS calibration.

2.6 Process Instrumentation

The furnace testing system contains several process instruments for monitoring moisture content, pressure, and temperature. The key instruments are as follows:

- Vaisala moisture monitor

- Panametrics moisture monitor

- MKS Baratron pressure transducers

- Cole-Parmer pressure transducers

- Type-K thermocouples.

2.6.1 Vaisala Moisture Monitor

The Vaisala moisture monitor model HMP230 uses the HUMIDICAP sensor. This sensor is based on a capacitance change of a thin polymer film as the film absorbs water. The sensor has a nominal dew point range of -40°C to 100°C. The probe tip is installed in the gas loop upstream of the furnace retort (see Figure 2.3). The sensor is designated as MT-01, and its integrated temperature sensor is designated as TT-01.

2.6.2 Panametrics Moisture Monitor

The Panametrics moisture monitor model MMS35 uses a solid electrochemical probe (model M2L) that measures moisture by measuring the characteristic capacitance of the probe as a function of the moisture in the gas phase. The sensor has a nominal dew point range of -110°C to 20°C. Previous testing indicated that contamination causes the probe to lose calibration and results in moisture readings that drift with time. To prevent contamination of the probe tip, the probe is installed in the gas loop downstream of two glass particulate filters. Further, the probes are changed following each test and surveyed for radioactive contamination. If no contamination is found, and the data correlate well with the data obtained from the MS, the readings are accepted.

A calibration verification procedure can be performed using calibrated water "leak" tubes. These tubes can be placed inside the furnace and, when heated, will establish a known water vapor pressure in

the system. However, this procedure is time intensive; approximately 2 weeks are required to calibrate one probe over the range of moisture likely to be encountered in these tests. This procedure is only used if the moisture monitor results vary widely from the MS data.

Output of the moisture monitor is in dew point (DP) in degrees Celsius. For comparison with other test data, these dew point values were converted to water vapor pressure in Torr using the water and ice vapor pressure data shown in Table 2.1. Interpolation of the data was accomplished using a 6th-order polynomial fit to the log of the vapor pressure (VP) versus temperature data. The resulting conversion expression is as follows:

$$VP \text{ (Torr)} = \log^{-1}[C_1 \cdot DP^6 + C_2 \cdot DP^5 + C_3 \cdot DP^4 + C_4 \cdot DP^3 + C_5 \cdot DP^2 + C_6 \cdot DP + C_7] \qquad (2.1)$$

where $C_1 = -6.7260E\text{-}12$
$C_2 = -1.7250E\text{-}09$
$C_3 = -1.7089E\text{-}07$
$C_4 = -7.2618E\text{-}06$
$C_5 = -2.9668E\text{-}04$
$C_6 = 3.4414E\text{-}02$
$C_7 = 6.5933E\text{-}01$

Table 2.1. Water and Ice Vapor Pressure Data Versus Temperature

Dew Point (°C)	Vapor Pressure (VP)		
	(Pa)[a]	(Torr)	Log (Torr)
-80	5.500E-02	4.126E-04	-3.385E+00
-75	1.220E-01	9.151E-04	-3.039E+00
-70	2.610E-01	1.958E-03	-2.708E+00
-65	5.400E-01	4.051E-03	-2.392E+00
-60	1.080E+00	8.101E-03	-2.091E+00
-55	2.093E+00	1.570E-02	-1.804E+00
-50	3.936E+00	2.952E-02	-1.530E+00
-45	7.202E+00	5.402E-02	-1.267E+00
-40	1.284E+01	9.631E-02	-1.016E+00
-35	2.235E+01	1.676E-01	-7.756E-01
-30	3.801E+01	2.851E-01	-5.450E-01
-25	6.329E+01	4.747E-01	-3.235E-01
-20	1.033E+02	7.746E-01	-1.109E-01
-15	1.653E+02	1.240E+00	9.339E-02
-10	2.599E+02	1.950E+00	2.899E-01
-5	4.018E+02	3.014E+00	4.791E-01
0	6.113E+02	4.585E+00	6.614E-01
10	1.228E+03	9.212E+00	9.644E-01
(a) CRC Press. 1997. *Handbook of Chemistry & Physics*, 78th edition.			

2.6.3 MKS Baratron Pressure Transducers

Two MKS Baratron model 690 calibrated pressure transducers coupled with MKS model 270 signal conditioners are used as the primary measurement for the overall system pressure. As shown in Figure 2.3, PE-01 measures the system pressure downstream of the retort outlet, whereas PE-06 measures the system pressure at the retort inlet. PE-01 indicates pressure in the range of 0.1 Torr to 10,000 Torr. The pressure range of PE-06 is 0.01 Torr to 1000 Torr. PE-06 was installed after the first two fuel element drying tests to provide more accurate measurements than PE-01 for low pressures. PE-06 is therefore considered the primary system pressure measurement. In addition, the 270 signal conditioner procured with PE-06 has a special capability to remotely zero the transducer, which provides more accurate pressure measurements below 1 Torr.

Two additional MKS Baratron units are also incorporated into the system, one to monitor the MS input pressure (see Section 2.5.1), and another to monitor the input pressure to the scroll pump.

An auxiliary high vacuum turbo pump is used to evacuate the inlet to PE-06 to well below 10^{-4} Torr so that the transducer can be accurately re-zeroed. The 270 signal conditioner used with PE-01 does not have a remote zeroing capability. Both signal conditioners have analog outputs that are interfaced to the DACS so that system pressure is continuously recorded.

2.6.4 Cole-Parmer Pressure Transducers

A Cole-Parmer model H-68801-53 diaphragm-type, calibrated pressure transducer is installed on the GC sample line as indicated by PE-08 in Figure 2.3. This pressure measurement is used to normalize the GC data so that actual gas concentrations in the system can be calculated from the relative concentrations measured. This sensor has a range of 0 to 1500 Torr with a resolution of 0.1 Torr and an accuracy of ±1% or ±1 Torr, whichever is larger. The readout unit (model H-68801-03) has an analog output that is interfaced to the DACS.

2.6.5 Thermocouples

Thermocouples provide a simple, reliable method for measuring system temperatures. As shown in Figure 2.3, over 20 thermocouples are installed at various locations in the system to provide key temperature measurements. The retort temperatures are of primary importance, and these temperatures are measured by thermocouples TE-04 through TE-10, which are positioned equidistant along the length of the retort. Other key temperature measurements include the retort center temperature (TE-20, which is a 30-in.-long thermocouple installed through the outlet end of the retort); retort inlet temperature (TE-21); condenser gas temperature (TE-19); and the condenser coolant temperature (TE-22). Thermocouples TE-11 through TE-17 are used for controlling the temperature of the heated lines. All thermocouple readings are continuously recorded using the DACS.

2.7 Data Acquisition and Control System

The DACS monitors system parameters and controls the furnace and the safety argon system. The DACS consists of a Hewlett Packard (HP) 3497A data acquisition/control unit, and an IBM-compatible computer. A National Instruments general-purpose interface bus card, installed in the IBM-compatible computer, is used to communicate with the HP 3497A. The computer communicates with the furnace temperature controllers over serial port 0 using an RS-232/RS-485 converter. The DACS uses National Instruments LabView for Windows as the control software.

The DACS is designed to measure critical system parameters during fuel conditioning tests, including temperatures, pressures, flow rates, and moisture level. The measured parameters are converted to engineering units, displayed on the computer screen, and stored to disk at user-defined intervals. The data files are stored in a tab-delimited format to allow importing into a standard spreadsheet or plotting program. A plotting screen also allows for plotting of up to six parameters at a time.

Limited control of the furnace can be performed with the DACS. Each of the three furnace zone temperatures can be remotely set by the DACS. In addition, the DACS allows the operator to start and stop the furnace and select one of four temperature profiles that are pre-programmed in the furnace temperature controllers. Note that these profiles must be programmed manually in the furnace controllers before using the DACS to select them.

3.0 Vacuum Drying Testing of Element 6513U

The drying test was performed in accordance with Test Procedure, *Furnace Testing of N-Reactor Fuel Element 6513U*, 3M-TWD-PTL-014, Revision 0. This document is located in the PNNL permanent project records for this test.

The testing consisted of three parts (discussed in this section):

- removing the fuel from its shipping canister, performing a visual inspection, loading the fuel onto the furnace system sample boat, and transferring it to the PTL G-Cell for loading into the furnace

- drying the fuel element using a combination of Cold Vacuum Drying (CVD) and Hot Vacuum Drying (HVD) processes

- unloading the furnace, performing a post-test visual inspection, and returning the fuel element to its shipping canister.

3.1 Fuel Element Transfer and Loading

3.1.1 Pre-Test Visual Inspection

The pre-test visual inspection was conducted using a high-resolution color CCD video camera located inside the PTL F-Cell (adjacent to the G-Cell), where the sample was unloaded from the shipping canister and visually inspected. The results were recorded using a Panasonic Super-VHS resolution video recorder. This examination was conducted to document the condition of the fuel element before the test and to determine if any changes had occurred since it was removed from the K-West Basin and shipped to the PTL. The results of this inspection are presented in Section 4.0.

3.1.2 Fuel Element Rinsing

Fuel element 6513U had been stored in the PTL water storage pool contained in a single fuel element canister (SFEC) that was filled with K-Basin water. The element was rinsed in F-Cell before the start of the drying test. This rinsing involved raising and lowering the element several times in the SFEC using one of the cell's manipulators. Following rinsing, the element was transferred to G-Cell for loading into the element test retort.

3.2 Fuel Element Drying

The fuel element was subjected to cold and hot vacuum drying. The drying test was conducted in six phases:

1. Cold Vacuum Drying
2. Pressure Rise Test
3. Hot Vacuum Drying (first step)
4. Hot Vacuum Drying (second step)
5. Hot Vacuum Drying (third step)
6. Post-Test Pressure Rise Test

The nominal design conditions used for these test phases are summarized in Table 3.1. Each phase is discussed below.

Table 3.1. Summary of Nominal Test Design Conditions

Test Segment	Nominal Test Condition[a]
A. Cold Vacuum Drying	
System Configuration	Pump on,[b] argon gas flow during initial condenser pumpdown phase
Test Temperature, °C	50
Atmosphere	Vacuum
Pressure, Torr	<5
Gas Flow Rate, cc/min	0 except during initial condenser phase
Gas Species Monitored	H_2, H_2O, N_2, O_2, CO_2, Ar, Kr, Xe
Duration, hr	CVD is conducted until the total pressure in the retort falls below 0.5 Torr.
B. Pressure Rise Test	
System Configuration	Test Chamber Isolated
Test Temperature, °C	50
Atmosphere	Vacuum
Initial Pressure, Torr	<5
Gas Flow Rate, cc/min	0
Pressure Rise (acceptable level, Torr)	<0.5
Duration, hr	1
C. Hot Vacuum Drying (Step 1)	
System Configuration	Pump on,[b] argon gas flow
Test Temperature Range, °C	75
Atmosphere	Vacuum, Ar background
Pressure, Torr	15
Gas Flow Rate, cc/min	300
Gas Species Monitored	H_2, H_2O, N_2, O_2, CO_2, Ar, Kr, Xe
Duration, hr	24

Table 3.1. (contd)

Test Segment	Nominal Test Condition[a]
D. Hot Vacuum Drying (Step 2)	
System Configuration	Pump on,[b] argon gas flow
Test Temperature Range, °C	75 to 400
Temperature Ramp Rate, °C/hr	10
Atmosphere	Vacuum, Ar background
Pressure, Torr	15
Gas Flow Rate, cc/min	300
Gas Species Monitored	H_2, H_2O, N_2, O_2, CO_2, Ar, Kr, Xe
Duration, hr	35
E. Hot Vacuum Drying (Step 3)	
System Configuration	Pump on,[b] argon gas flow
Test Temperature, °C	400
Atmosphere	Vacuum, Ar background
Pressure, Torr	15
Gas Flow Rate, cc/min	300
Gas Species Monitored	H_2, H_2O, N_2, O_2, CO_2, Ar, Kr, Xe
Duration, hr	10
F. Cooldown	
System Configuration	Pump on,[b] argon gas flow
Test Temperature, °C	400 to 50
Atmosphere	Vacuum
Initial Pressure, Torr	15
Gas Flow Rate, cc/min	300
Gas Species Monitored	H_2, H_2O, N_2, O_2, CO_2, Ar, Kr, Xe
Duration, hr	~100
G. Pressure Rise Test	
System Configuration	Test Chamber Isolated
Test Temperature, °C	50
Atmosphere	Vacuum
Initial Pressure, Torr	<5
Gas Flow Rate, cc/min	0
Duration, hr	1
(a) Nominal test design conditions. Actual values are given in the text.	
(b) Vacuum pump was throttled during the drying test.	

3.2.1 Cold Vacuum Drying

While the fuel element was being handled and prepared for the drying test, it was kept damp by sprinkling it with deionized water. The amount of surplus liquid water, though small, could not be ascertained. There were no pools of water in the sample boat; however, water was adsorbed into corroded areas, cracks, and crevices. An additional ~10 ml of water were added to the sample boat just before loading it into the furnace to ensure sufficient free water in the system prior to CVD.

The furnace was first purged with argon to remove as much air as possible. The furnace was then isolated and the furnace temperature increased to approximately 50°C and allowed to stabilize. After stabilization, argon flow was re-established; the system vacuum pump was turned on (in a throttled mode); and the system water condenser was valved in. When the system pressure became lower than the condenser could extract, the condenser was valved out of the gas loop and the argon flow stopped. The remainder of the CVD was conducted with the throttled vacuum pump. CVD was conducted at an ultimate pressure of ~0.7 Torr for ~20 hr. The purpose of the CVD portion of the test was to determine if CVD is successful in removing the majority of the free water from the system in a reasonable length of time.

During the condenser pump-out phase of CVD, uranium hydride has the potential to be formed through the reaction

$$U + \frac{3}{2}H_2 \rightarrow UH_3 \tag{3.1}$$

The activation energy for this reaction has a negative enthalpy (Condon and Larson 1973) at low partial pressures and also negative entropy (Manchester and San-Martin 1995). At these partial pressures, the reaction rate is somewhat pressure dependent (Bloch and Mintz 1981). These thermodynamic data suggest that the formation of uranium hydride is favorable under CVD conditions.

3.2.2 Pressure Rise Test

The Pressure Rise Test involved isolating the system and measuring any pressure increase while at CVD pressure and temperature conditions. The purpose of the Pressure Rise Test was to determine the effectiveness of the preceding CVD process. This test was conducted by valving the vacuum pump out of the gas loop and closing the exhaust valves. The condition for acceptance of this portion of the test was a total system pressure rise of less than 0.5 Torr in a 1-hr time period. If this condition was not met, the system was re-opened to the vacuum pump and the Pressure Rise Test repeated.

3.2.3 Hot Vacuum Drying, Step 1

Following completion of the Pressure Rise Test, the vacuum pump was re-opened to the system retort; argon gas flow was established at a rate of ~304 sccm; and the retort temperature was increased to ~75°C. This condition was held for a period of ~19 hr. This portion of the test can be used to obtain isothermal hydrogen and water release data for assessing oxidation of the fuel at low temperatures.

3.2.4 Hot Vacuum Drying, Step 2

The second step of the HVD process involved raising the temperature of the retort from ~75°C to ~400°C at a carefully controlled rate while maintaining the same argon flow and pressure conditions. Thus, any release of gas species during this temperature rise could be assigned to a specific temperature. The second step of HVD was conducted for about 35 hr.

During this step, hydrogen may be released from the fuel through the decomposition of uranium hydride (Cotton 1988); this reaction is rapid at temperatures greater than 250°C:

$$UH_3 \rightarrow U + \frac{3}{2}H_2 \tag{3.2}$$

Water may also be liberated by various hydrated species found on fuel elements, such as hydrates of uranium oxides, aluminum hydroxides, and hydrated iron oxides. Water is also released slowly along a "tortuous path" from beneath corroded parts of the fuel element and from behind the cladding. The released water can react with the fuel element to generate hydrogen through the reactions:

$$U + 2H_2O \rightarrow UO_2 + 2H_2 \tag{3.3}$$

$$UH_3 + 2H_2O \rightarrow UO_2 + \frac{7}{2}H_2 \tag{3.4}$$

3.2.5 Hot Vacuum Drying, Step 3

The final step of the HVD process involved holding the temperature of the retort at ~400°C while again maintaining the same argon flow and pressure conditions as in steps 1 and 2. This step will yield isothermal release data for any remaining hydrated species on the fuel element and for oxidation of uranium by any remaining water. This final step of the HVD process was conducted for about 21 hr.

3.2.6 System Cooldown and Post-Test Pressure Rise Test

Following completion of the final HVD step, the system retort was allowed to cool to ~50°C while maintaining the same vacuum and flow conditions, and then another Pressure Rise Test was conducted to determine the baseline in-leakage rate of air into the retort from the cell environment. Knowing this rate is important to allow for correction of the system and moisture pressure increase rates determined in the initial post-CVD Pressure Rise Test. Since the conditions for the post-HVD test are identical to those used for the initial test, the assumption is made that the air in-leakage rate should be nearly the same as well.

3.3 Calculation of Water and Hydrogen Inventories

Assuming ideal gas behavior of the water vapor, total water inventory (m) in the system during those portions of the test conducted with argon flowing into the retort can be approximated from the measured water vapor pressure and the argon gas flow as follows:

$$\frac{dm}{dt} = \frac{M}{V_0} \cdot \frac{P_w}{(P_t - P_w)} \cdot \frac{dV}{dt} \qquad (3.5)$$

where dm/dt is the rate of water removal in grams per minute, M is the molecular mass of water in grams per mole, dV/dt is the flow rate in liters per minute (at the calibration temperature of 0°C), V_0 is the molar volume of gas at 0°C and 1 atmosphere in liters per mole, P_w is the partial pressure of water vapor in Torr, and P_t is the total pressure in Torr. The total amount of water released is given by integrating the rate data over time.

The hydrogen inventory may be calculated in a similar fashion with the $[P_w/(P_t-P_w)]$ expression in the above equation replaced with the measured atom fraction of hydrogen. For the purposes of this report, all hydrogen data are plotted in Torr·l rather than grams. At the calibration conditions of the argon flow controller, 1 Torr·l is equivalent to approximately 0.12 mg of hydrogen.

The assumptions made in estimating the water and hydrogen values are:

- The flow into the retort is approximately equal to the flow out (i.e., contributions to the flow from other gas species such as hydrogen are neglected).

- The argon mass flow is referenced to 25°C (as determined from the calibration of the flow gauges).

- The sample gas is at the same temperature as the calibration gas (GC and MS measurements).

4.0 Visual Examinations of Element 6513U

4.1 Fuel Element Description and Background

An N-Reactor fuel assembly consists of an inner element and outer element made from a uranium alloy co-extruded with a Zircaloy-2 cladding. Both elements are annular, right-cylinders. The inner element has a smaller outer diameter and is held in place within the outer element.

Fuel element 6513U, chosen for Run 8, was an outer element removed from the K-West Basin in 1996. The element had been in sealed water storage in the K-West Basin since 1983. This fuel element was selected to represent a classification of fuel damage termed "severely damaged" (Lawrence 1997). The furnace drying test series (of which Run 8 was added to the original 7 tests) were intended to progress from intact (unbreached) fuel elements to severely damaged fuel elements. This fuel element was the second "severely damaged" fuel element tested.

The fuel element had been kept in K-Basin water at the PTL storage basin since it was loaded into its SFEC and shipped to the facility in 1996. The first relatively detailed examination of the fuel element was conducted just before the drying test and is discussed below.

4.2 Pre-Test Visual Inspection

The fuel element was removed from its SFEC and examined using a CCD color video camera in the PTL F-Cell. The fuel element was split along the length in several places and damaged on both ends. One end was only moderately cracked and damaged, the other severely damaged with the end cap attached to the fuel element by a small strip of cladding. This end cap (which still had some of the uranium fuel matrix attached) broke away from the fuel element during handling in the PTL.

Figure 4.1 shows a still image of the less-damaged end of the fuel element. This end was located at the bottom of the K-West storage canister while the fuel element was at the K-West Basin. Figure 4.2 shows the more-damaged end and separated end cap. The end cap was included in the drying test. This fuel element was also breached and cracked along the sides (longitudinal axis). Figure 4.3 shows one of the breached areas along the side of the fuel element. As with previous cracked/broken elements, water within the cracks wicked to the surface during the visual examination. This water is visible as the darker regions decorating the crack area.

Like most of the fuel elements used in these drying tests, this element appeared to have a thin, light-gray-colored coating on the surface. As in the other tests, no attempt was made to recover this material, since experience has shown that a large amount of surface would have to be "scrubbed" to gather an adequate sample for analysis.
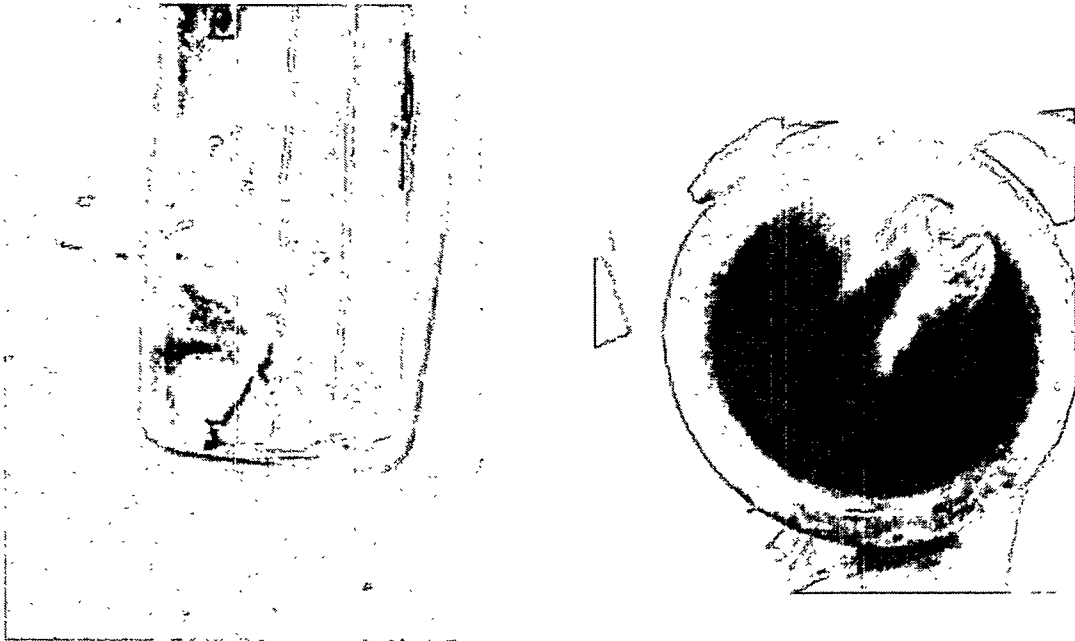
Figure 4.1. Side and End View of the Less-Damaged Portion of Fuel Element 6513U Prior to the Drying Test. Some of the fuel matrix was missing beneath the cracked area (most likely due to corrosion).

Figure 4.2. Side and End View of the More-Damaged Portion of Fuel Element 6513U Prior to the Drying Test. The end cap piece had some of the fuel matrix attached. This element had large areas of fuel voiding due to in-basin corrosion.
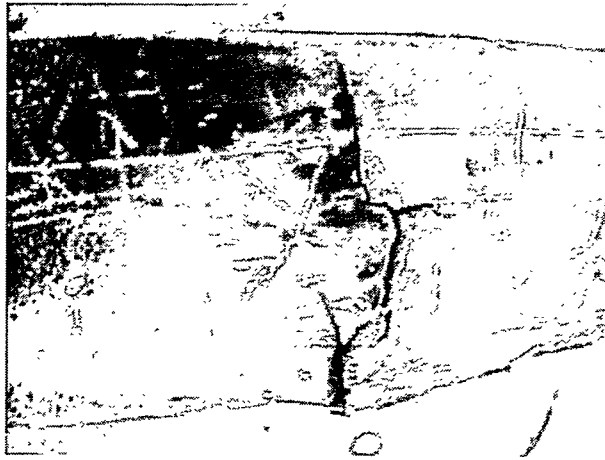
Figure 4.3. Fuel Element Breach Located Near the Middle of Fuel Element 6513U

4.3   Post-Test Visual Examination

Similar to the fuel elements tested in Runs 4 (Element 5744U), 5 (Element 6603M), 6 (Element 1164M), and 7 (Element 2660M), the fuel element surface coloration changed from a light gray color to a dark color. As discussed in the results from those tests, this could be due to the transformation of uranium oxy-hydrates releasing water and leaving behind simpler oxide phases. Some oxides are known to be dark in color, as observed on the fuel element.

Similar to the other tests, some of the fuel element cracks broadened as a result of the drying test. The drying process used for this test, as in all the tests conducted as part of this test series, involved several stages and included a step during which the fuel element was heated to 400°C. It is uncertain during which stage the cladding cracks opened further. It was possible to view the fuel matrix under the cladding cracks in some places. The fuel matrix appeared similar to fuel elements 5744U, 6603M, and 2660M from Runs 4, 5, and 7 respectively. It did not appear "rubbleized" as was observed for fuel element 1164M tested in Run 6. Figure 4.4 shows a view of a crack that had opened further during the drying test.

This test was different from the other tests in that some of the cracks did not open further during drying. Although the reason for this will likely be unresolved, it can be speculated that there was less water in these cracks or perhaps some other reason the fuel in this region did not oxidize sufficiently to push open the cladding. This observation could also suggest the crack opening process is due to stress relaxation in the cladding as a result of the heating process rather than a result of fuel oxidation. Figure 4.5 shows a view of the same region shown in Figure 4.3 (although rotated about 45 degrees). The post-drying crack does not appear to be different in appearance from the pre-drying condition.

From the visual examination results, this fuel element can be grouped with those elements tested in Runs 4, 5, and 7. As in those runs, the fuel element may be classified as "severely damaged" but may not be that severe in terms of overall fuel surface area or percentage of cracks that are postulated to hold much of the uranium hydride inventory.

4.3

Figure 4.4. Photomosaic Showing a Crack Along the Side of Fuel Element 6513U Following the Drying Test. This crack appeared to have opened slightly during drying.
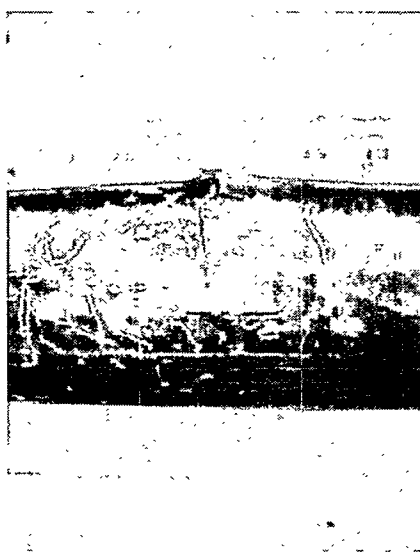

Figure 4.5. Post-Test Image of the Same Region Shown in Figure 4.3. The crack is not noticeably different.

5.0 Experimental Results

In the following sections, the experimental data collected during the drying test are expanded and plotted for each segment. Summary results from the test are plotted in Figure 5.1. This figure shows the system moisture-level response to the pressure changes and the retort tube temperatures during the test. Time intervals for the various test segments are shown in the upper section of the plot and are also outlined in Table 5.1. The temperatures shown in Figure 5.1 were recorded from one of seven thermocouples (TE-07) on the system located near the center of the retort. The pressure data were taken from the 0 to 1000 Torr Baratron sensor (PE-06) located upstream of the retort. Small moisture variations evident during the cooldown phase are due to temperature fluctuations in the cell area of the PTL.

5.1 Cold Vacuum Drying

The water release from the CVD portion of the test is shown in Figure 5.2. The baseline moisture partial pressure in the system before heating was ~6 Torr at a retort temperature of ~24°C. Total system pressure was ~750 Torr, with no argon gas flow. After heating to ~50°C, the moisture pressure and system pressure stabilized at ~5 Torr and ~836 Torr, respectively. Assuming ideal gas behavior, the pressure after heating is approximately 20 Torr higher than expected. This excess pressure has been observed in all the previous tests, except for the first dry-run, and may have been due to gases evolved during the heatup, such as hydrogen from moisture reactions and gases dissolved in the free water. Another explanation for the calculated pressure difference is that the average retort temperature was somewhat greater than 50°C.

The CVD phase started at an elapsed time (ET) of 200 min. Figure 5.2 shows that the moisture pressure rose almost immediately to ~10 Torr, followed by a relatively steady decrease over the remainder of CVD. A small jump in the moisture pressure at an ET of ~300 min coincides with isolation of the condenser and cessation of argon gas flow. Pumping was continued by the throttled vacuum pump alone. By the end of CVD (ET = 1380), the moisture pressure had dropped to ~0.2 Torr, and the total pressure had dropped to ~0.5 Torr.

Approximately 6 ml of water were observed in the condenser during the CVD phase. Calculated water removal during the time period when the condenser was open under argon flow yielded a value of ~3 g, somewhat lower than the water observed in the condenser. Approximately 10 ml of water were added at the start of the test, in addition to any water remaining on the element from the initial element rinsing. The reason for the under-recovery of water in the condenser may be due to hang-up of water in colder sections of the system, particularly the particulate filters. Review of previous drying test data shows good correlation of fractional water recovery versus duration of the condenser pumpdown phase. Run 7 (Element 2660M), which had a much longer condenser phase, showed significantly higher fractional water recovery.
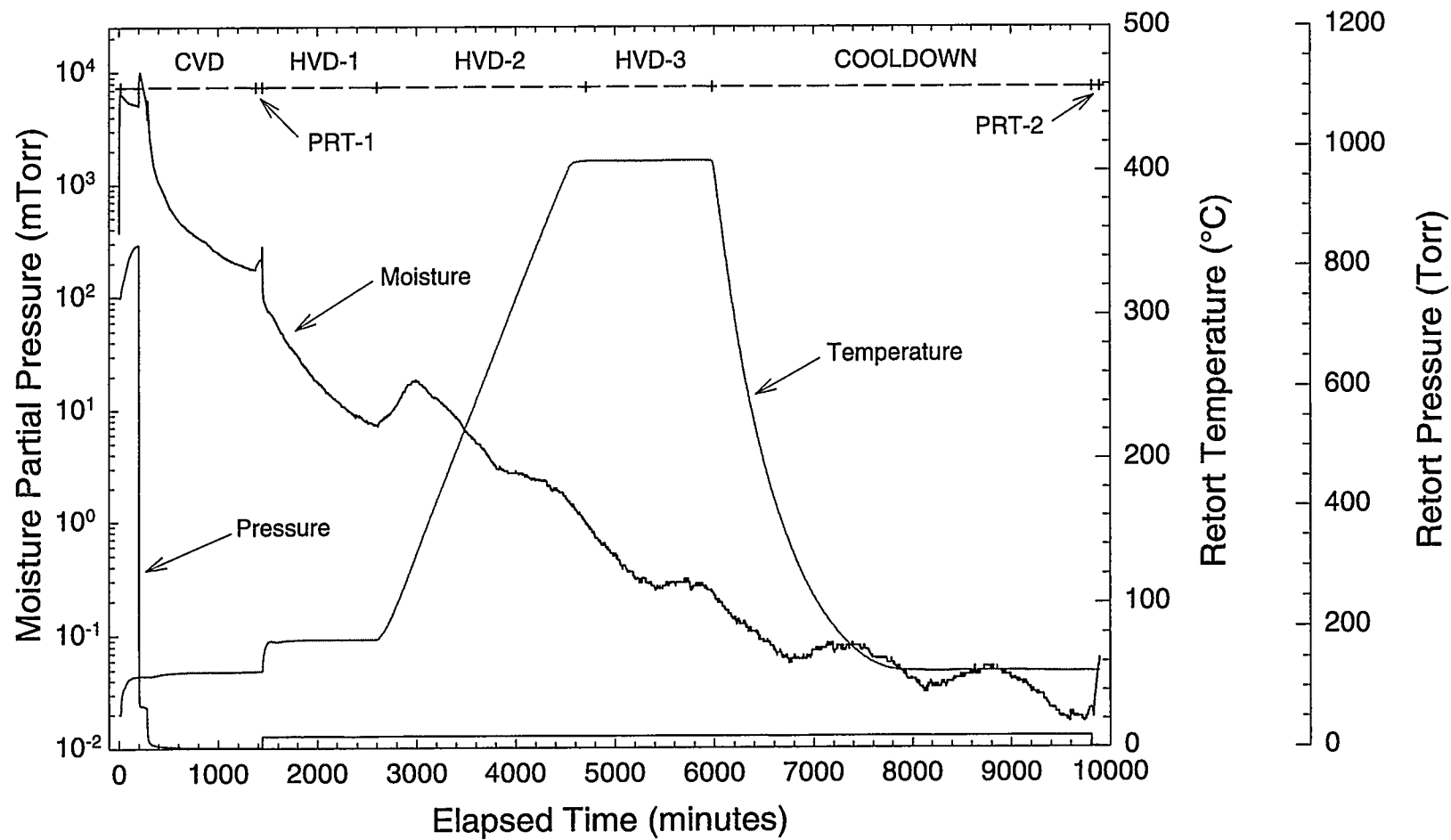
Figure 5.1. Drying of SNF Element 6513U, Summary Plot

Table 5.1. Fuel Element 6513U Drying Run Time Line

| Activity	Date/Time	Elapsed Time (min)
Start of Test		
Heat furnace to ~50°C	06/01/98 15:03	17
Cold Vacuum Drying Test		
Open pump[a] and condenser (initial), start argon flow	06/01/98 18:05	200
Open pump, close condenser (final), stop argon flow	06/01/98 19:30	284
Pressure Rise Test		
Close pump (isolate furnace)	06/02/98 13:46	1380
Open pump valve	06/02/98 14:51	1445
Hot Vacuum Drying Test (Step 1)		
Start argon flow (~300 sccm), raise furnace temperature to ~75°C and hold	06/02/98 14:52	1446
Hot Vacuum Drying Test (Step 2)		
Raise furnace temperature to ~400°C @ 10°C/min	06/03/98 10:05	2600
Hot Vacuum Drying Test (Step 3)		
Hold furnace temperature at ~400°C	06/04/98 18:35	4550
System Cooldown		
Reduce temperature of retort to ~50°C, maintain argon flow	06/05/98 18:24	5979
Post-Test Pressure Rise Test		
Turn off argon flow and close pump valve (isolate furnace)	06/08/98 10:19	9814
Turn off furnace heaters, end test	06/08/98 11:34	9889
(a) The vacuum pump was throttled for the drying test.		
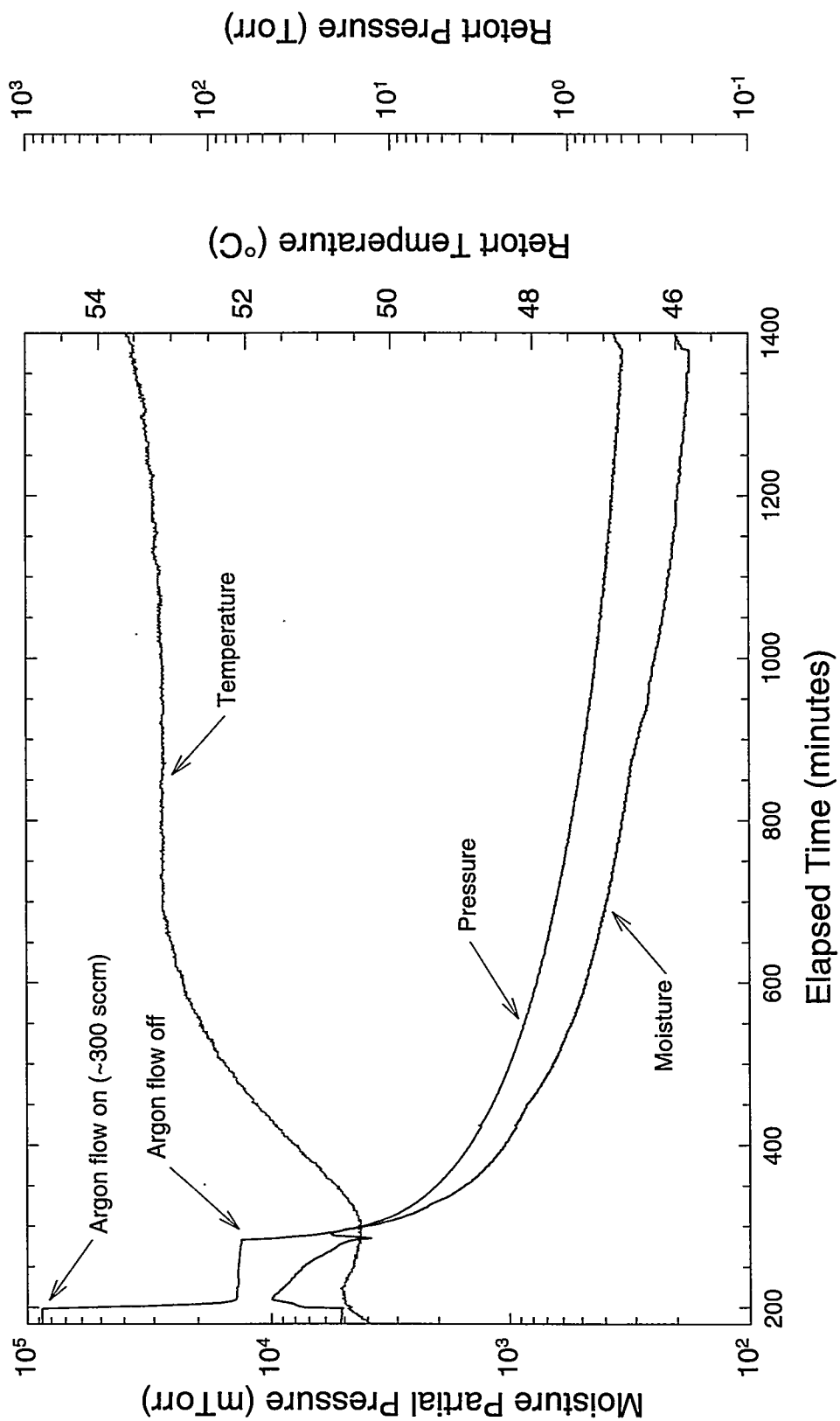
Figure 5.2. Drying of SNF Element 6513U, Cold Vacuum Drying

5.4

5.2 Pressure Rise Tests

The results of the two pressure rise phases of the drying test (post-CVD and post-HVD) are shown in Figures 5.3 and 5.4. As discussed earlier, the purpose of the post-HVD test was to determine as best as possible the ambient air in-leakage rate into the system as it had been configured for the drying test. While under vacuum conditions, with no argon flow, any air in-leakage will contribute to the data signals observed for the various process gases measured during the test, particularly water and hydrogen (from oxidation). The data plotted for the total pressure are from the 0 to 1000 Torr Baratron sensor (PE-06) located upstream of the retort. This sensor has higher sensitivity and therefore lower noise than the 0 to 10,000 Torr Baratron (PE-01) located downstream of the retort. To calculate the total water mass removed from the retort, however, pressure data from the 0 to 10,000 Torr sensor were used, as this sensor is closer to the moisture sensor. Differences in the pressure indications of the two sensors are generally small; however, for the present test, there was some observed variation in the pressure indication of PE-01 during the latter phase of CVD. Since there was no argon flow during this period, this variation had no effect on any calculated water removal values.

The post-CVD Pressure Rise Test was conducted over an ET of 1380 min to 1445 min. Both the total pressure and the moisture pressure showed nearly linear pressure rises over the course of the test. Regression fits (dotted lines in the figure) yielded a total pressure rise rate of ~0.12 Torr/hr (well below the 0.5 Torr/hr criterion for the test), and a moisture pressure rise rate of ~0.027 Torr/hr.

Assuming that the water vapor pressure increase is from water sources within the test system, and assuming ideal gas behavior of the water vapor, the rate of desorption of the water (dn/dt) will be given by

$$\frac{dn}{dt} = \frac{V}{RT} \cdot \frac{dP}{dt}$$

(5.1)

where n is the number of moles of gas, V is the volume of the system (~10,000 cm^3), R is the gas constant (82.06 cm^3·atm/g-mol·K), T is the temperature (~326 K), and dP/dt is the rate of change in the pressure given by the slope of the regression line. The total amount of water released to the system during the Pressure Rise Test is given by the integral of the above equation and was ~0.3 mg. Assuming a total surface area of ~8900 cm^2 for the system (total surface area of the retort, sample boat, tubing, and an outer fuel element), and 10^{15} atoms per cm^2 as the monolayer gas density on surfaces, approximately one monolayer equivalent of H$_2$O was evaporated.

The results of the post-HVD pressure rise measurements are shown in Figure 5.4. Again, both the total pressure and the moisture pressure show essentially linear increases with time, however with significantly lower slopes than observed earlier for the post-CVD test. The total pressure rise has a regression slope of ~0.003 Torr/hr, and the moisture pressure rise has a slope of ~0.000043 Torr/hr. The rate of increase in the total pressure is about a factor of 10 lower than the lowest pressure increase seen
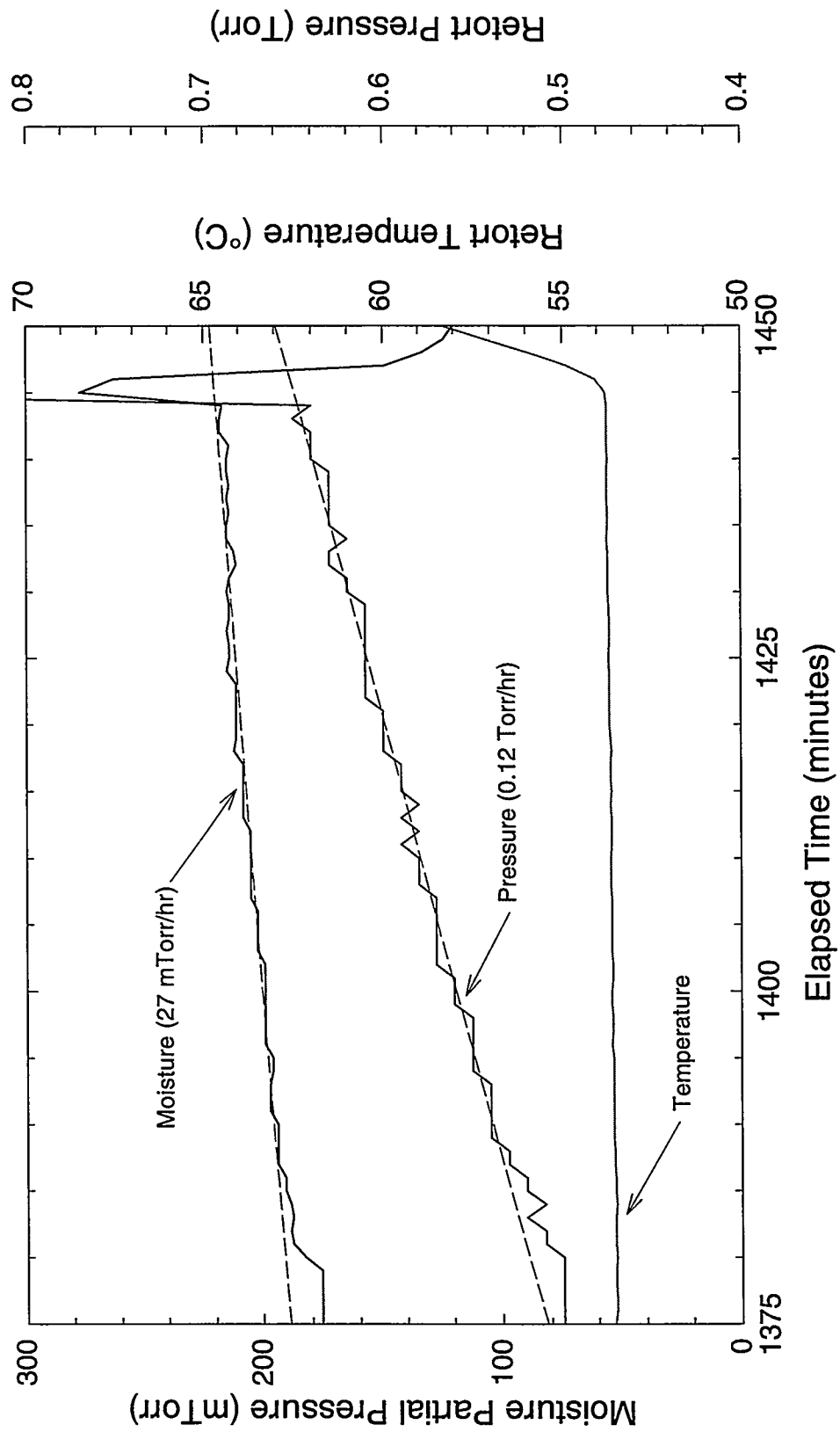
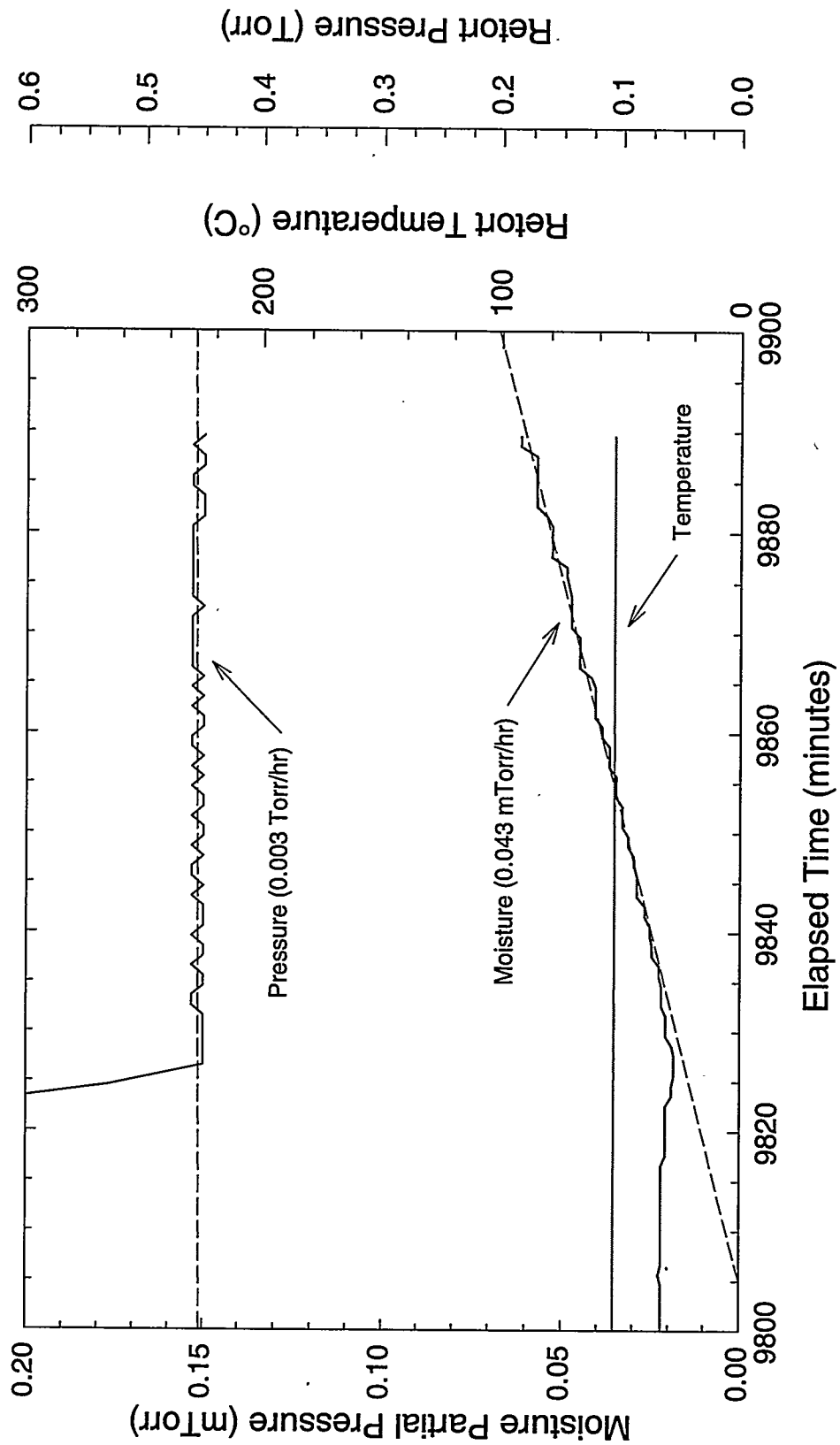**Figure 5.3.** Drying of SNF Element 6513U, Post-CVD Pressure Rise Test

5.6

Figure 5.4. Drying of SNF Element 6513U, Post-HVD Pressure Rise Test

5.7

(~0.04 Torr/hr for Run 5, Element 6603M) since this measurement was included in the test protocol for Run 3 (Element 0309M). This would suggest that the final sealing condition of the retort was significantly improved over earlier tests.

The ratio of the water pressure rise to the total pressure is ~0.014, somewhat higher than would be expected just from humidity alone in air in-leakage from the cell environment (air at 20°C and 25% relative humidity would yield a water pressure-to-total pressure ratio of ~0.007), suggesting some contribution from residual water in the test system.

Comparing the pressure data from the two Pressure Rise Tests indicates that the total pressure rise observed in the initial post-CVD test is only partially caused by residual moisture and/or air in-leakage. The difference between the total pressure rise and the moisture pressure rise for the post-CVD test (~0.093 Torr/hr) is significantly higher than can be explained by air in-leakage into the retort alone as measured in the post-HVD test (~0.003 Torr/hr). This suggests that other sources of gas, such as hydrogen, are responsible for some of the observed total pressure rise in the post-CVD test.

5.3   Hot Vacuum Drying

The first segment of HVD, shown in Figure 5.5, includes the ramp and hold from ~50°C to ~75°C in flowing argon gas (~300 sccm) under partial vacuum. HVD-1 occurred over an ET of 1446 min to 2600 min. The moisture pressure decreased steadily from ~150 mTorr to ~7 mTorr during the ~75°C phase. Total system pressure was essentially constant over this first HVD phase at ~19 Torr. Total water removed was ~0.6 g.

The second HVD phase involved maintaining the same system conditions as in HVD-1, but raising the temperature slowly from ~75°C to ~400°C at a rate of 10°C/hr. HVD-2 occurred over an ET of 2600 min to 4550 min and is shown in Figure 5.6. During the temperature rise, the moisture pressure increased, showing a distinct peak at ~134°C (~18 mTorr), with smaller peaks at ~345°C (~2 mTorr) and possibly at ~170° (~13 mTorr). As has been observed in previous tests, these peaks are an indication of water release from chemisorbed sites (i.e., hydrated species). Total water removed during the second phase of HVD was ~0.3 g, about one half of that removed during the first phase. Total system pressure was essentially constant at ~19 Torr.

The third phase of HVD is shown in the left-hand side of Figure 5.7 (ET of 4550 min to 5979 min) and covered the temperature hold period at ~400°C. This period is characterized by a steady decrease in the moisture pressure from ~3 mTorr to ~0.2 mTorr. Total water removed was ~14 mg.

Following the final HVD phase, the system was allowed to cool to ~50°C in preparation for the post-test Pressure Rise Test discussed above. Water removed during the system cooldown was ~4 mg. Total system pressure remained constant at ~19 Torr during HVD-3 and cooldown.
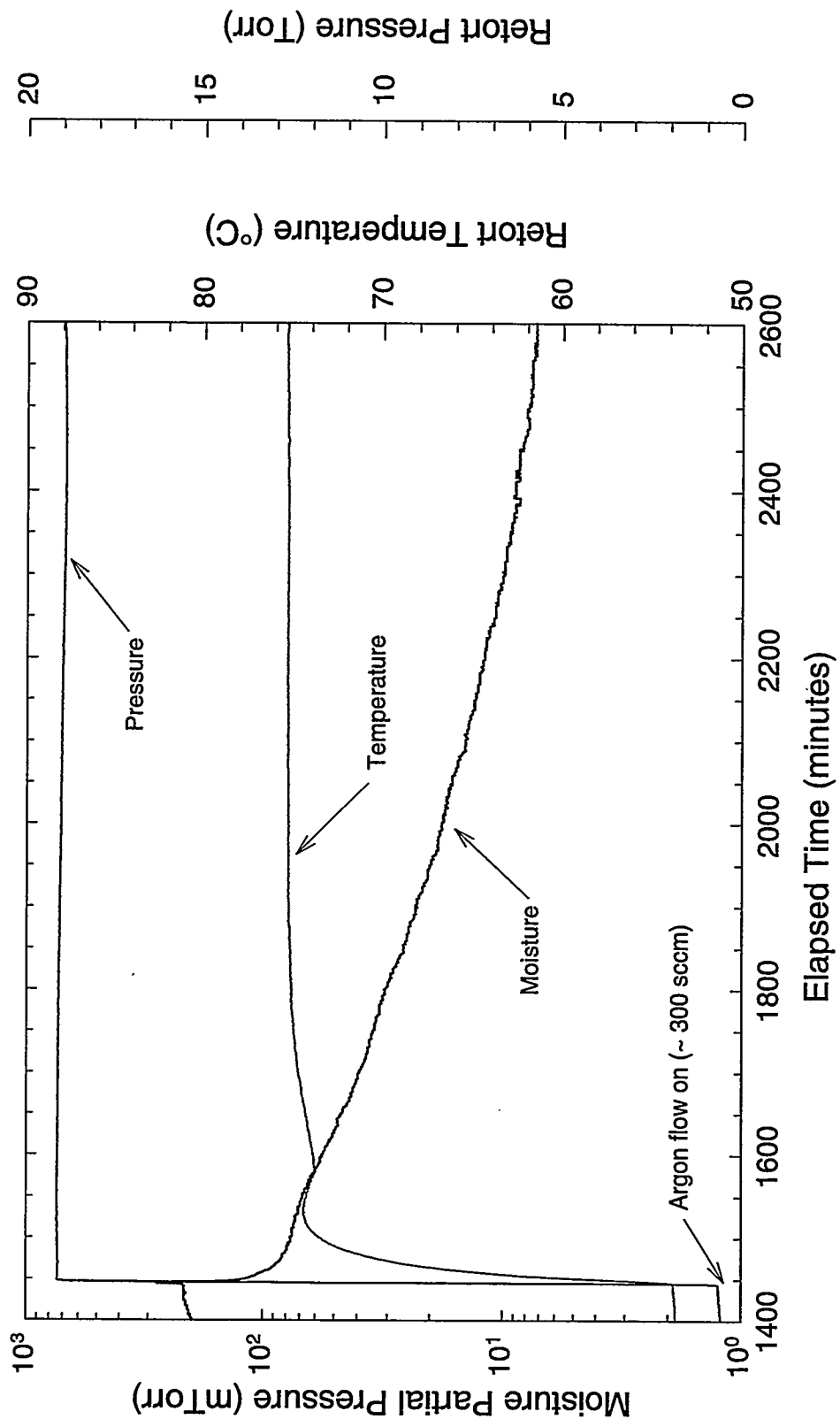
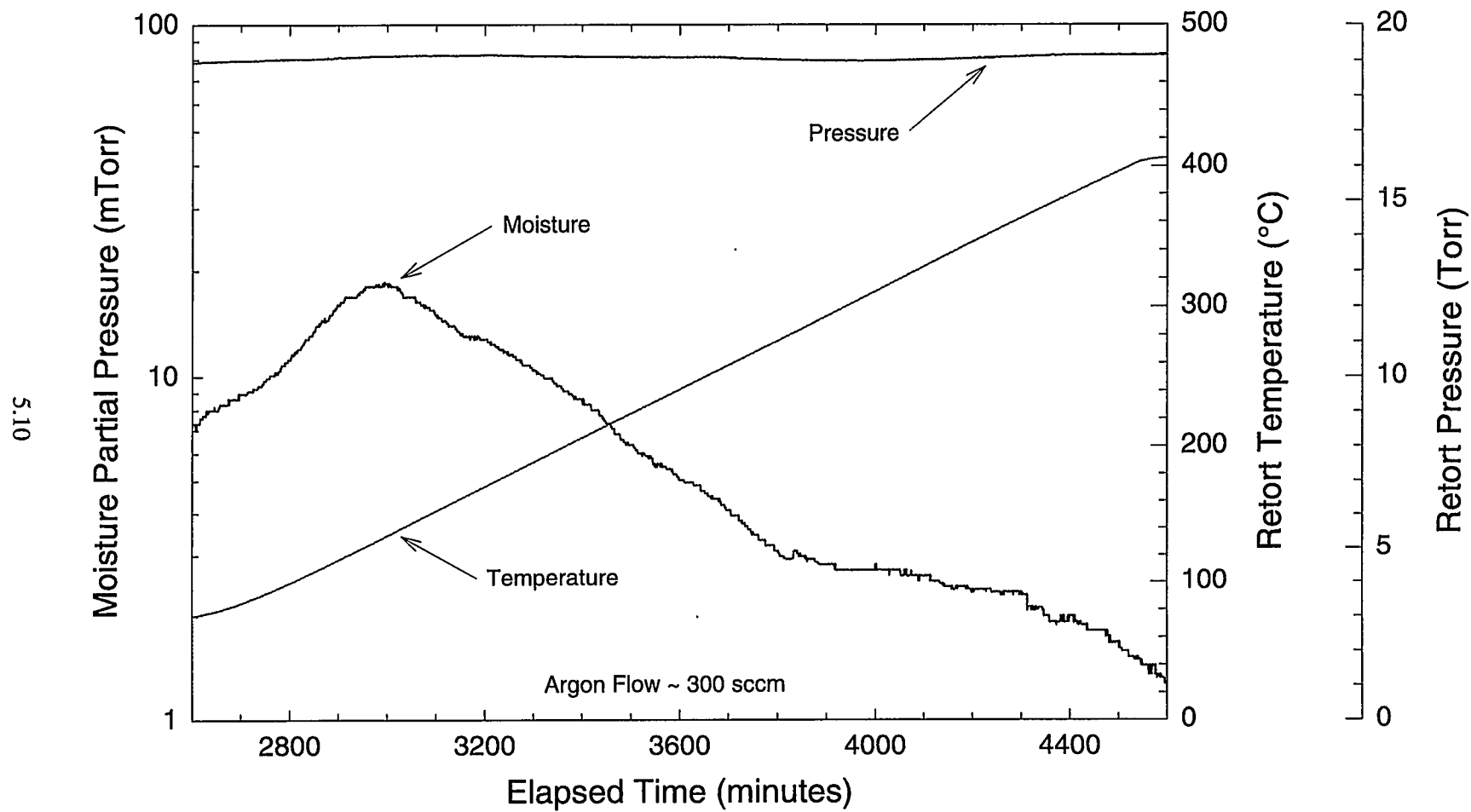**Figure 5.5.** Drying of SNF Element 6513U, Hot Vacuum Drying – Step 1

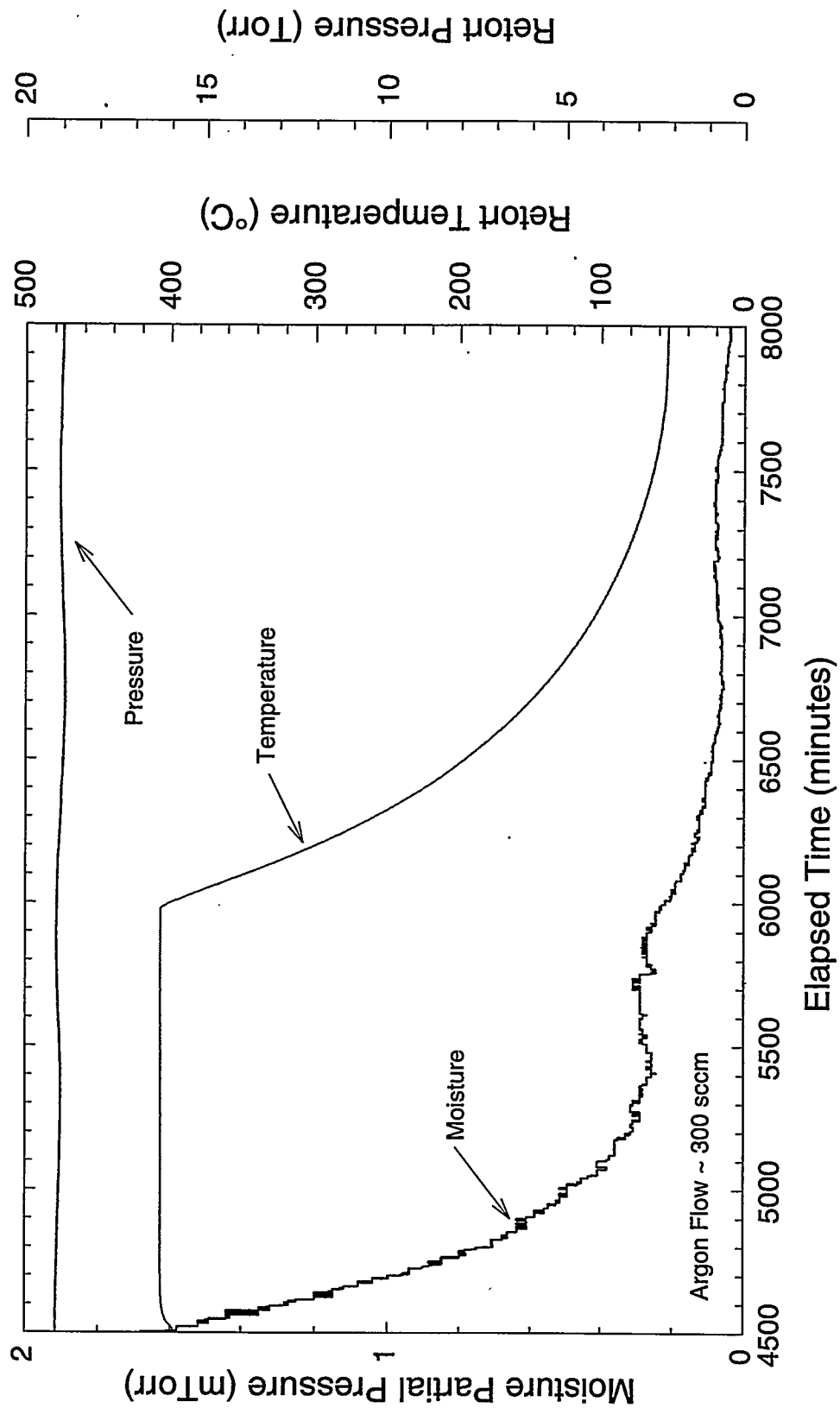**Figure 5.6.** Drying of SNF Element 6513U, Hot Vacuum Drying – Step 2

Figure 5.7. Drying of SNF Element 6513U, Hot Vacuum Drying – Step 3

5.11

5.4 Gas Chromatograph Measurements

The GC was used to measure hydrogen in the sample gas during a portion of the CVD step and during the HVD step when argon was flowing through the system. To determine the location of the hydrogen peaks during HVD and the integrated amounts of hydrogen involved with each peak, the HVD hydrogen data were deconvoluted using a commercial peak-fitting computer program, PeakFit. A five-parameter asymmetrical fitting function (Pearson IV) was used to fit each of the separate deconvoluted peaks.

Hydrogen data collected during the condenser pumpdown phase of CVD are shown in Figure 5.8. Hydrogen values during this phase closely followed the moisture signal, peaking at ~0.4 Torr·l/min (ET ~213 min) before dropping to ~0.2 Torr·l/min at the end of the condenser phase of CVD. Total hydrogen release during this period was ~26 Torr·l (~3 mg). In term of moles, the relative water-to-hydrogen amounts generally ranged from ~70 to ~100, indicating that about 1% of the available water released during CVD reacted with the fuel to produce hydrogen. As discussed earlier, some of the released hydrogen may also have reacted with the fuel to produce uranium hydride.

Measured hydrogen release during the HVD segments of the drying test is shown in Figure 5.9. Four peaks are associated with the hydrogen release. The first occurred during the initial phase of HVD at ~75°C at an ET of ~1738 min. This peak was characterized by a fairly rapid rise in the hydrogen signal, followed by a slow approximately exponential decay. From deconvolution of the hydrogen data, ~149 Torr·l (~17 mg) of hydrogen were released during HVD-1. The three remaining peaks occurred during HVD-2 at temperatures of ~148°C, ~208°C, and ~257°C. Approximately 1900 Torr·l (~220 mg) of hydrogen were released during the entire HVD process, over a time period of ~75 hours, with the majority being released during HVD-2.

As noted in Section 3.2.3, HVD-1 is isothermal except for the initial temperature ramp from ~50°C to ~75°C and can, therefore, be used to provide information on reaction kinetics. During HVD-1, the hydrogen signal first increases and then later decreases steadily with time. By contrast, the water signal decreases steadily with time during HVD-1. This behavior has been observed in earlier runs and suggests that oxidation is occurring during the initial part of HVD-1 as the bulk of the fuel element reaches 75°C, with the oxidation slowing in the latter phases of HVD-1 in concert with the drop in available moisture.

The hydrogen peaks at ~148°C and ~208°C during the early part of HVD-2 roughly correlate with the large water release peak occurring slightly earlier. Approximately 735 Torr·l (~86 mg) of hydrogen and ~200 mg of water were released during this time period. It is likely that the hydrogen released during this period was due to oxidation of fuel by water released through oxy-hydrate decomposition in the corrosion regions or in isolated regions under the cladding. The molar ratio of water to hydrogen released was ~0.28, indicating that about 80% of the water released from the fuel by decomposition over this time period reacted with the fuel. In previous drying tests, similar fractions have been observed.
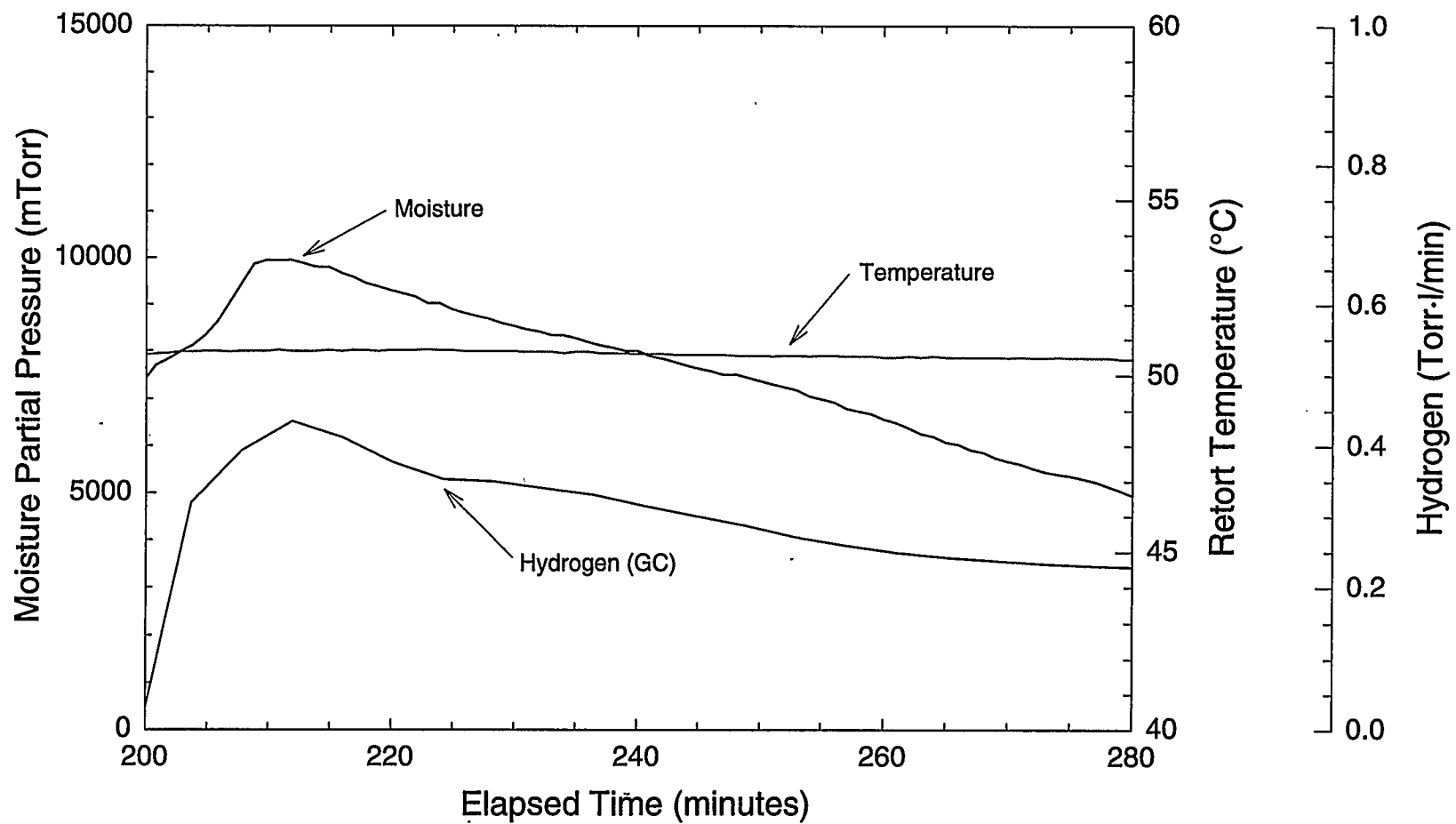
5.12

Figure 5.8. Drying of SNF Element 6513U, Hydrogen Release During CVD
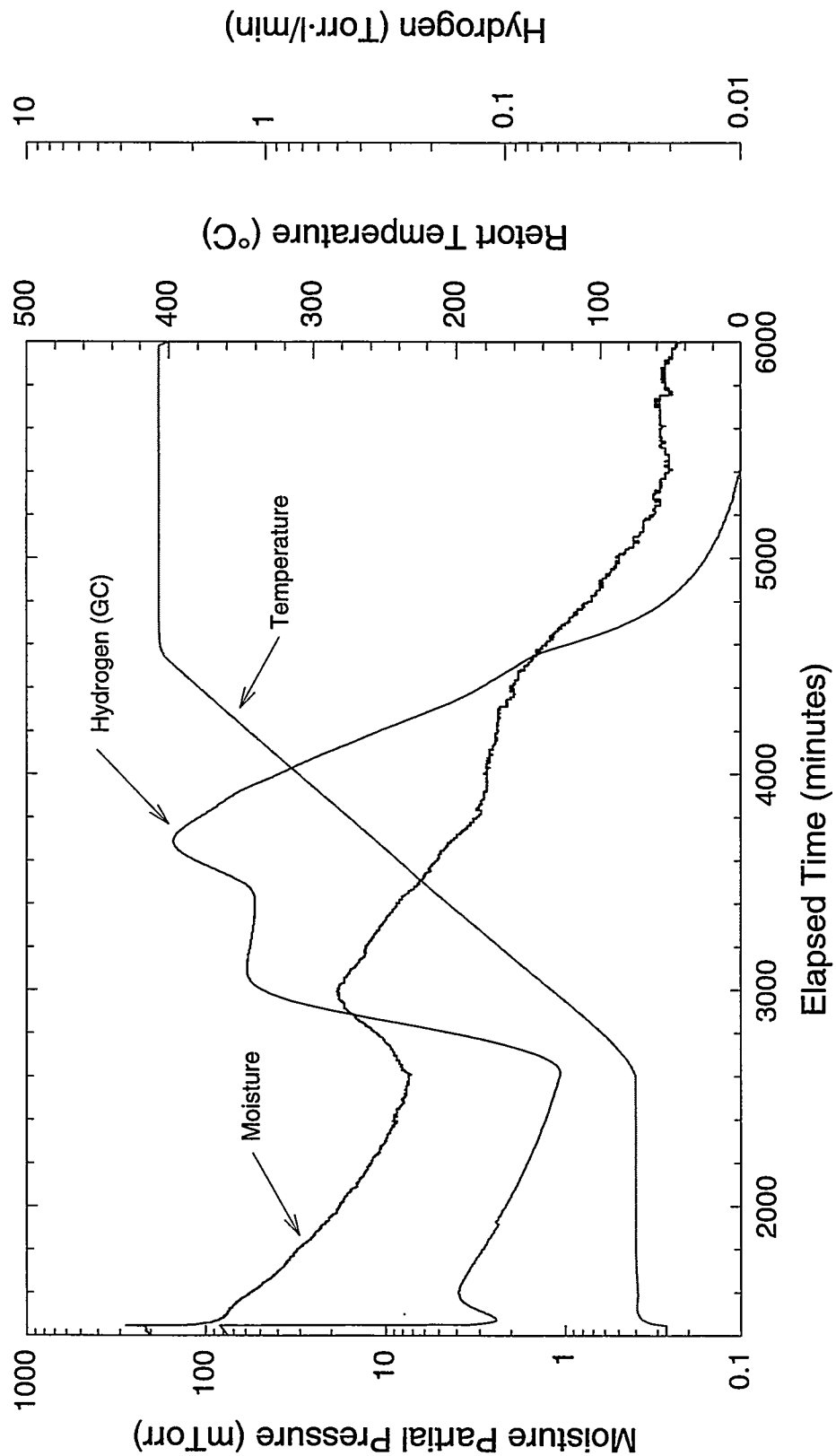
Figure 5.9. Drying of SNF Element 6513U, Hydrogen Release During HVD and Cooldown

5.14

The 257°C peak accounted for the majority of the hydrogen release, amounting to ~990 Torr·l (~116 mg). This peak was most likely due to the decomposition of uranium hydride since there is little UH₃ correlation with the water signal during this period. Also, this temperature is close to the expected temperature for UH₃ decomposition (Cotton 1988). This quantity of hydrogen would represent ~9 g of decomposition. The total quantity of hydrogen released during the HVD-2 phase was ~1700 Torr·l (~200 mg).

5.5 Mass Spectrometer Measurements

The drying system was designed so that the Balzers Omnistar MS could be used in conjunction with the GC to collect hydrogen and other gas release data over the test run. Because of continued technical problems with the MS, however, only short sections of MS data were collected; thus, no MS data are presented for this test. Earlier tests, however, have shown good correlation between the GC and MS hydrogen data.

6.0 Discussion

Ten milliliters of water were added to the element boat prior to the test. Of this, approximately 6 ml of water were observed in the condenser during the condenser pumpdown phase of CVD, somewhat higher than that calculated (~3 g) from Equation 3.4 over the same time period. The reason for the under-recovery of water in the condenser may be due to hang-up of water in colder sections of the system, particularly the particulate filters. Review of previous drying test data shows good correlation of fractional water recovery versus duration of the condenser pumpdown phase.

An additional ~0.3 mg of water was removed during the post-CVD Pressure Rise Test. This release can likely be interpreted as coming from free water that was trapped and not completely released during CVD. Approximately 10 ml of water were added to the system prior to the start of the test. Similar to earlier tests, the total pressure rise observed in the post-CVD test was only partially caused by residual moisture, suggesting that other sources of gas are responsible for some of the total pressure rise observed in the post-CVD test.

During the first segment of HVD, approximately 0.6 g of water was removed at temperatures between ~50°C and ~75°C. The second phase of HVD released approximately 0.3 g of water with a main peak at ~134°C. The final phase of HVD at 400°C released only about 14 mg of water, with an additional ~4 mg of water released during post-HVD cooldown. Consistent with previous tests, this indicates that small residual quantities of water remained even after the drying test was completed.

Most of the water removal after the post-CVD Pressure Rise Test occurred during the first phase of HVD, which entailed the temperature ramp from ~50°C to ~75°C. This water release is attributed largely to the release of water from regions beneath the cladding and from under the corroded regions, although decomposition of metal oxy-hydrates may also account for some of this water. Therefore, water released from the element from isolated regions along a "tortuous path" may be the controlling factor in post-CVD water removal. The peaks in the moisture release during HVD-2 indicate water release from chemisorbed sites (i.e., hydrated species) at higher temperatures. As observed in previous drying tests, a temperature above 400°C may be required for complete drying of the fuel element within a reasonable period of time.

Hydrogen data were obtained from the GC during the condenser pumpdown phase of CVD and during HVD. During the CVD period, approximately 3 mg of hydrogen were released, indicating that about 1% of the available water released during CVD is reacted with the fuel to produce hydrogen. The hydrogen partial pressure was well correlated with the water partial pressure during this time. Thermodynamic data suggest that the formation of uranium hydride is favorable under CVD conditions.

During HVD, hydrogen was first observed starting at the ramp-up to ~75°C, reaching a peak at ~0.2 Torr·l/min before slowly decreasing. From deconvolution of the hydrogen data, ~149 Torr·l (~17 mg) of hydrogen were released during HVD-1, attributed to oxidation of the fuel by remaining free water. Hydrogen release increased again during the ramp from ~75°C to ~400°C, with three noticeable peaks at ~148°C, ~208°C, and ~257°C. The first two peaks roughly correlate with a similar water release

6.1

and amount to ~735 Torr·l (~86 mg). It is likely that this hydrogen release is due to oxidation of fuel by water released through oxy-hydrate decomposition. The latter hydrogen release peak (~990 Torr·l or ~116 mg) at ~257°C is likely due to uranium hydride decomposition and is equivalent to ~9 g of UH_3 decomposed. Above ~257°C, the level of hydrogen decreased rapidly with time, with ~23 Torr·l (~2.7 mg) of hydrogen released during HVD-3. Total hydrogen release during HVD was ~1900 Torr·l (~220 mg), roughly comparable to that observed for fuel elements 5744U (Run 4) and 2660M (Run 7).

Because of technical problems, no useful MS data were collected during the run. Earlier tests, however, have shown good correlation between the GC and MS hydrogen data.

7.0 References

Bloch, J., and M. H. Mintz. 1981. *Journal of the Less Common Metals* 81:301-320.

Condon, J. B., and E. A. Larson. 1973. *The Journal of Chemical Physics* 59(2):855-865.

Cotton, F. A. 1988. *Advanced Inorganic Chemistry*, 5th Edition. John Wiley & Sons, New York.

CRC Press. 1997. *Handbook of Chemistry and Physics*, 78th Edition. New York.

Lawrence, L. A. 1997. *Strategy for Examination of the 15 K-West Basin Fuel Elements*. HNF-SD-SNF-SP-018, DE&S Hanford, Inc., Richland, Washington.

Manchester, F. D., and A. San-Martin. 1995. *Journal of Phase Equilibria* 16(3):263-275.

Ritter, G. A., S. C. Marschman, P. J. MacFarlan, and D. A. King. 1998. *Whole Element Furnace Testing System*. PNNL-11807, Pacific Northwest National Laboratory, Richland, Washington.

Westinghouse Hanford Company (WHC). 1995. *Hanford Spent Nuclear Fuel Project Integrated Process Strategy for K Basins Spent Nuclear Fuel*. WHC-SD-SNF-SP-005, Rev. 0, Richland, Washington.

8.0 Supporting Documents and Related Reports

Gerry, W. M. 1997a. *Calibration of Mass Flow Controllers*. SNF-TP-012, Rev. 0, Pacific Northwest National Laboratory, Richland, Washington.

Gerry, W. M. 1997b. *Calibration of Balzer Quadstar Mass Spectrometer*. SNF-TP-014, Rev. 0, Pacific Northwest National Laboratory, Richland, Washington.

Gerry, W. M. 1997c. *Calibration of MTI Gas Chromatograph Model M200*. SNF-TP-013, Rev. 0, Pacific Northwest National Laboratory, Richland, Washington.

Serles, J. A. 1997. *Furnace Testing of N-Reactor Fuel Element 6513U*. 3M-TWD-PTL-014, Rev. 0, Pacific Northwest National Laboratory, Richland, Washington.

Reports are written separately for the whole element drying test series as follows:

System Design Description for the Whole Element Furnace Testing System

Spent Fuel Drying System Test Results (First Dry-Run)

Spent Fuel Drying System Test Results (Second Dry-Run)

Spent Fuel Drying System Test Results (Dry-Run in Preparation for Run 8 [Third Dry-Run])

Drying Results of K-Basin Fuel Element 1990 (Run 1)

Drying Results of K-Basin Fuel Element 3128W (Run 2)

Drying Results of K-Basin Fuel Element 0309M (Run 3)

Drying Results of K-Basin Fuel Element 5744U (Run 4)

Drying Results of K-Basin Fuel Element 6603M (Run 5)

Drying Results of K-Basin Fuel Element 1164M (Run 6)

Drying Results of K-Basin Fuel Element 2660M (Run 7)

Drying Results of K-Basin Fuel Element 6513U (Run 8)

Distribution

No. of
Copies

No. of
Copies

OFFSITE

C. L. Bendixsen
Idaho National Engineering and
  Environmental Laboratory
P.O. Box 1625
Mail Stop 3135
Idaho Falls, ID 83415

A. W. Conklin
Washington State Department of Health
Airdustrial Park
Building 5, Mail Stop LE-13
Olympia, WA 98504-0095

M. A. Ebner
Idaho National Engineering and
  Environmental Laboratory
P.O. Box 1625
Mail Stop 3114
Idaho Falls, ID 83415

A. R. Griffith
U.S. Department of Energy, Headquarters
19901 Germantown Rd (EM-65)
Germantown, MD 20585-1290

T. J. Hull
U.S. Department of Energy, Headquarters
19901 Germantown Road (EH-34)
Germantown, MD 20874-1290

M. R. Louthan
Savannah River Technology Center
Materials Technology Center
Aiken, SC 29808

T. E. Madey
Rutgers University
Bldg. 3865
136 Freylinghuysen Rd
Piscataway, NJ 08854

B. K. Nelson
U.S. Department of Energy, Headquarters
19901 Germantown Road (EM-65)
Germantown, MD 20874-1290

R. G. Pahl, Jr.
Argonne National Laboratory
P. O. Box 2528
Idaho Falls, ID 83403

R. S. Rosen
Lawrence Livermore National Laboratory
20201 Century Blvd., 1ST Floor
Germantown, MD 20874

D. Silver
Washington State Department of Ecology
P.O. Box 47600
Olympia, WA 98504-7600

T. A. Thornton
Yucca Mountain Project M&O Contractor
SUM1/423
1261 Town Center Drive
Las Vegas, NV 89134

No. of
Copies

ONSITE

6 DOE Richland Operations Office

R. M. Hiegel	S7-41
P. G. Loscoe	S7-41
C. R. Richins	K8-50
E. D. Sellers	S7-41
J-S. Shuen	S7-41
G. D. Trenchard	S7-41

22 Duke Engineering and Services,
Hanford, Inc.

C. B. Aycock	R3-11
R. B. Baker	H0-40
D. W. Bergmann	X3-79
S. A. Chastain	H0-40
D. R. Duncan	R3-86
J. R. Frederickson	R3-86
L. H. Goldmann	R3-86
S. L. Hecht	H0-40
B. J. Makenas	H0-40
A. L. Pajunen	R3-86
R. W. Rasmussen	X3-85
A. M. Segrest	R3-11
J. A. Swenson	R3-11
C. A. Thompson	R3-86
D. J. Trimble (5)	H0-40
D. J. Watson	X3-79
J. H. Wicks, Jr.	X3-74
SNF Project Files	R3-11

3 Fluor Daniel Hanford

E. W. Gerber	R3-11
D. A. Smith	T4-13
M. J. Wiemers	R3-11

No. of
Copies

2 Fluor Daniel Northwest

L. J. Garvin	R3-26
G. A. Ritter	H0-40

7 Numatec Hanford Company

G. P. Chevrier	H5-25
T. Choho	R3-86
E. R. Cramer	H0-34
T. A. Flament	H5-25
J. J. Irwin	R3-86
C. R. Miska	R3-86
J. P. Sloughter	H5-49

2 Technical Advisory Group

J. C. Devine	R3-11
R. F. Williams	R3-11

32 Pacific Northwest National Laboratory

J. Abrefah (7)	P7-27
J. P. Cowin	K8-88
S. R. Gano	K2-12
W. J. Gray	P7-27
B. D. Hanson	P7-27
G. S. Klinger	P7-22
D. K. Kreid	K7-80
P. J. MacFarlan	P7-27
S. C. Marschman (5)	P7-27
B. M. Oliver	P7-22
R. P. Omberg	K7-80
T. M. Orlando	K8-88
L. R. Pederson	K2-44
J. K. Tarantino	K9-41
J. C. Wiborg	K7-74
Information Release (7)	